On the connectivity of the cosmic web

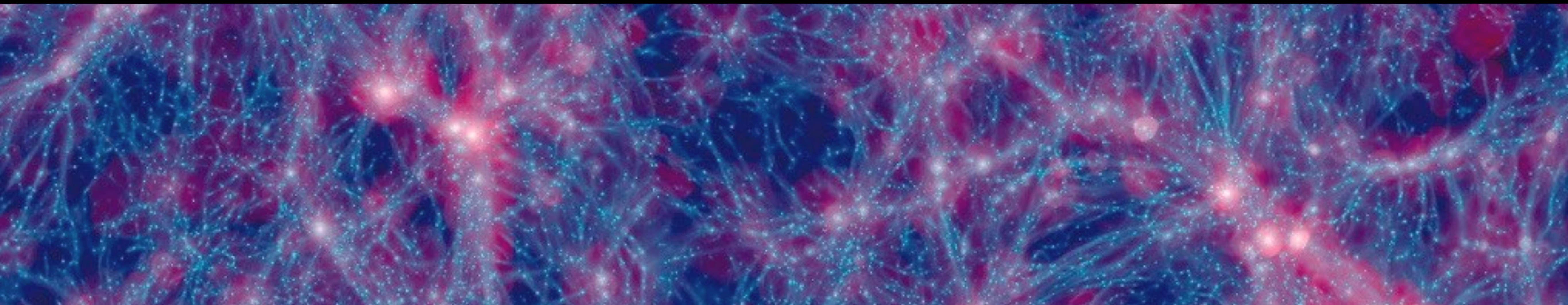

Sandrine Codis

- Institut d'Astrophysique de Paris -

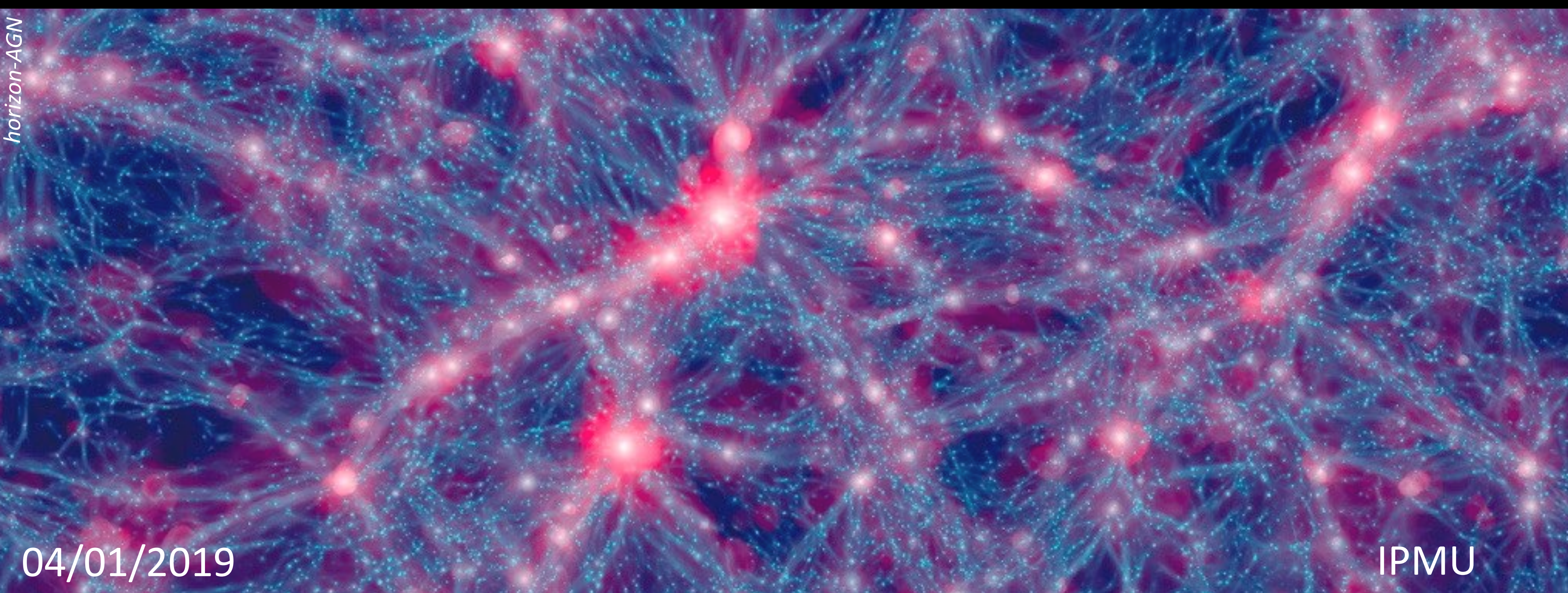

04/01/2019

IPMU

On the connectivity of the cosmic web

- Birth and growth of the cosmic web
- Random fields, Peak theory, topology
- Cosmic connectivity

How is the cosmic web woven?

Gaussian primordial fluctuations

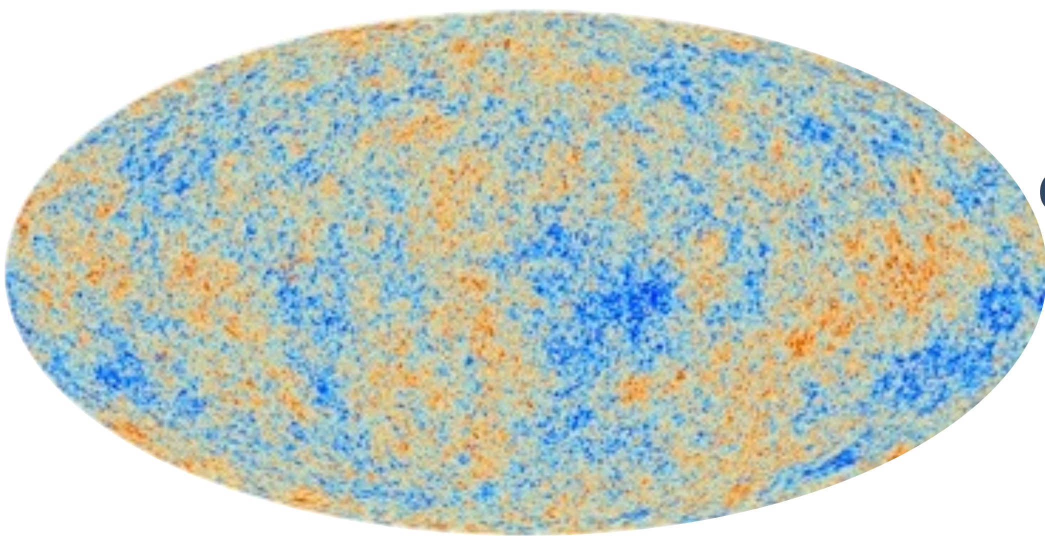

Gravitational instability

expansion

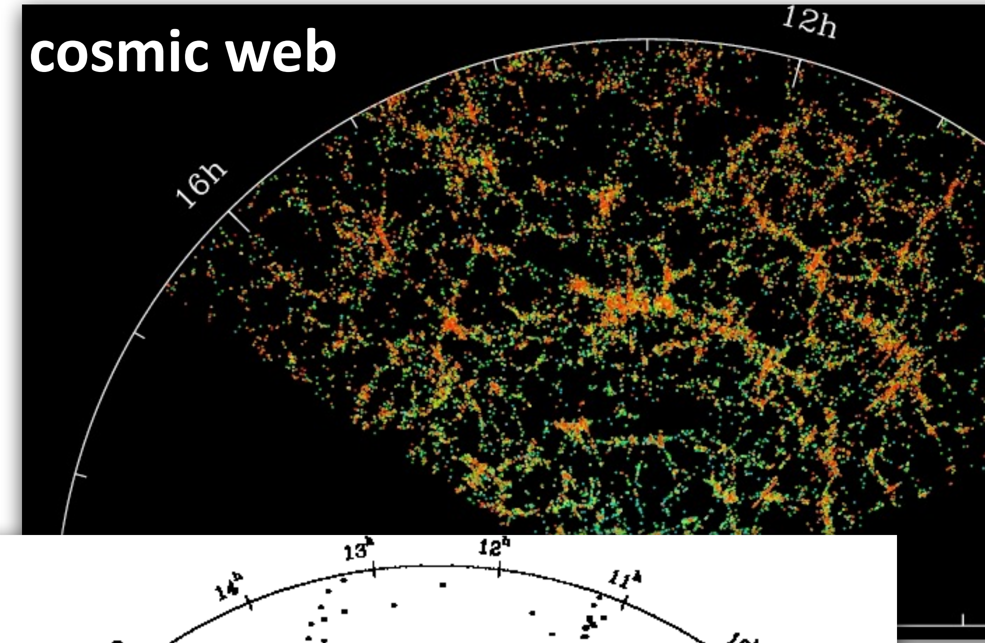

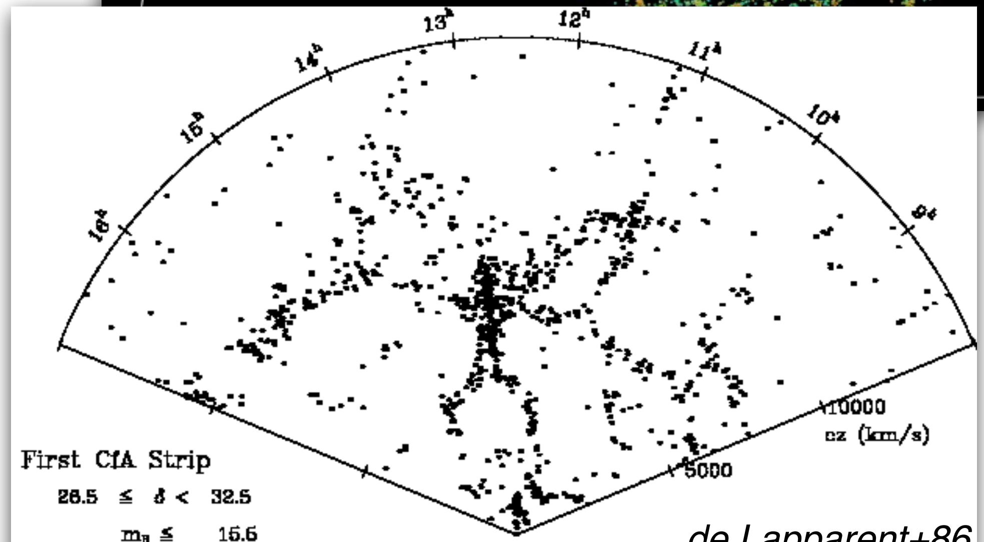

de Lapparent+86

Vlasov-Poisson equations: dynamics of a self-gravitating collisionless fluid

Liouville theorem:

$$\left[\frac{\partial}{\partial t} + \frac{\mathbf{p}}{ma^2}\frac{\partial}{\partial \mathbf{x}} - m\nabla\phi\frac{\partial}{\partial \mathbf{p}}\right] f(\mathbf{x},\mathbf{p},\mathbf{t}) = \mathbf{0}$$

Poisson equation:

$$\Delta\phi = 4\pi a^2 G(\rho - \bar{\rho})$$

These highly non-linear equations can be solved using numerical simulations or analytically in some specific regimes. Exact solutions are crucial to understand the details of structure formation.

Before shell-crossing, moments>2 can be neglected (velocity dispersion,...) and we get evolution equations for the cosmic density and velocity fields:

continuity equation:

$$\frac{\partial \delta}{\partial t} + \frac{1}{a}\nabla\cdot[(1+\delta)\mathbf{u}] = 0$$

Euler equation:

$$\frac{\partial u_i}{\partial t} + \frac{\dot{a}}{a}u_i + \frac{u_j\partial_j u_i}{a} = -\frac{\partial_i\phi}{a} - \frac{\partial_j[\rho\sigma_{ij}]}{\rho a}$$

Poisson equation:

$$\Delta\phi = 4\pi a^2 G(\rho - \bar{\rho})$$

Anisotropic dynamics within the cosmic web:
Matter escapes from voids to sheets, filaments and ends up in nodes.

DM simulation by C. Pichon

Anisotropic dynamics within the cosmic web:
Matter escapes from voids to sheets, filaments and ends up in nodes.

DM simulation by C. Pichon

Anisotropic dynamics within the cosmic web: Matter escapes from voids to sheets, filaments and ends up in nodes.

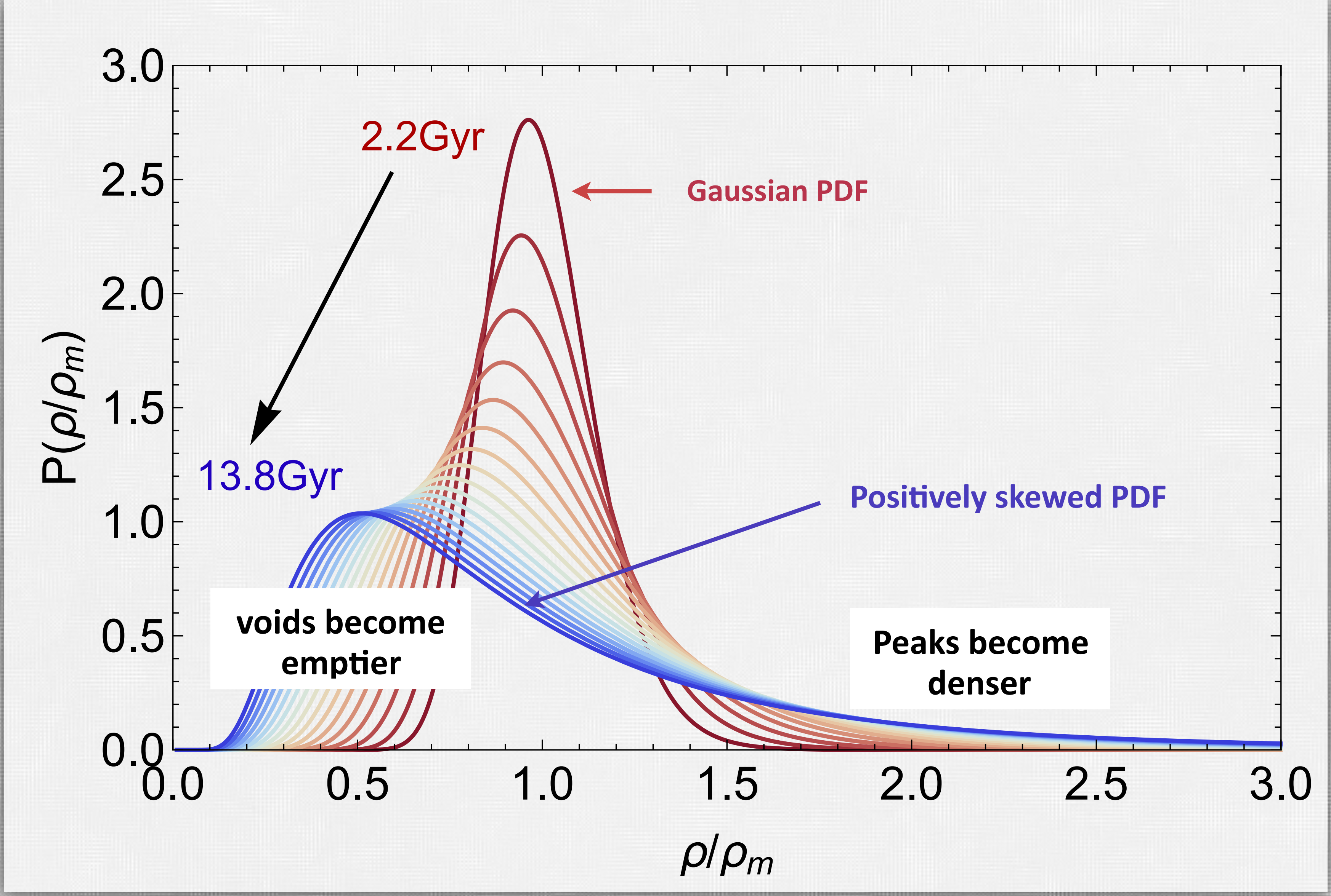

DM simulation by C. Pichon

Vlasov-Poisson equations: dynamics of a self-gravitating collisionless fluid

Liouville theorem:

$$\left[\frac{\partial}{\partial t} + \frac{\mathbf{p}}{ma^2}\frac{\partial}{\partial \mathbf{x}} - m\nabla\phi\frac{\partial}{\partial \mathbf{p}}\right] f(\mathbf{x},\mathbf{p},\mathbf{t}) = \mathbf{0}$$

Poisson equation:

$$\Delta\phi = 4\pi a^2 G(\rho - \bar{\rho})$$

These highly non-linear equations can be solved using numerical simulations or analytically in some specific regimes. Exact solutions are crucial to understand the details of structure formation.

Before shell-crossing, moments>2 can be neglected (velocity dispersion,…) and we get evolution equations for the cosmic density and velocity fields:

continuity equation:

$$\frac{\partial\delta}{\partial t} + \frac{1}{a}\nabla\cdot[(1+\delta)\mathbf{u}] = 0$$

Euler equation:

$$\frac{\partial u_i}{\partial t} + \frac{\dot{a}}{a}u_i + \frac{u_j\partial_j u_i}{a} = -\frac{\partial_i\phi}{a} - \frac{\partial_j[\rho\sigma_{ij}]}{\rho a}$$

Peebles 1980; Fry 1984; Bernardeau 2002

Poisson equation:

$$\Delta\phi = 4\pi a^2 G(\rho - \bar{\rho})$$

Vlasov-Poisson equations: dynamics of a self-gravitating collisionless fluid

Liouville theorem:

$$\left[\frac{\partial}{\partial t} + \frac{\mathbf{p}}{ma^2}\frac{\partial}{\partial \mathbf{x}} - m\nabla\phi\frac{\partial}{\partial \mathbf{p}}\right] f(\mathbf{x},\mathbf{p},\mathbf{t}) = \mathbf{0}$$

Poisson equation:

$$\Delta\phi = 4\pi a^2 G(\rho - \bar{\rho})$$

These highly non-linear equations can be solved using numerical simulations or analytically in some specific regimes. Exact solutions are crucial to understand the details of structure formation.

Before shell-crossing, moments>2 can be neglected (velocity dispersion,…) and we get evolution equations for the cosmic density and velocity fields:

continuity equation:

$$\frac{\partial \delta}{\partial t} + \frac{1}{a}\nabla \cdot [(1+\delta)\mathbf{u}] = 0$$

Euler equation:

$$\frac{\partial u_i}{\partial t} + \frac{\dot{a}}{a}u_i + \frac{u_j \partial_j u_i}{a} = -\frac{\partial_i \phi}{a} - \cancel{\frac{\partial_j [\rho\sigma_{ij}]}{\rho a}}$$

Peebles 1980; Fry 1984; Bernardeau 2002

Poisson equation:

$$\Delta\phi = 4\pi a^2 G(\rho - \bar{\rho})$$

From Eulerian to Lagrangian space

Eulerian pt of view:
- Fixes the frame
- Fields on a grid
- δ, u
- « volume-weighted statistics »

Lagrangian pt of view:
- Follows the fluid
- Particules
- $x=q+\psi$
- « mass-weighted statistics »

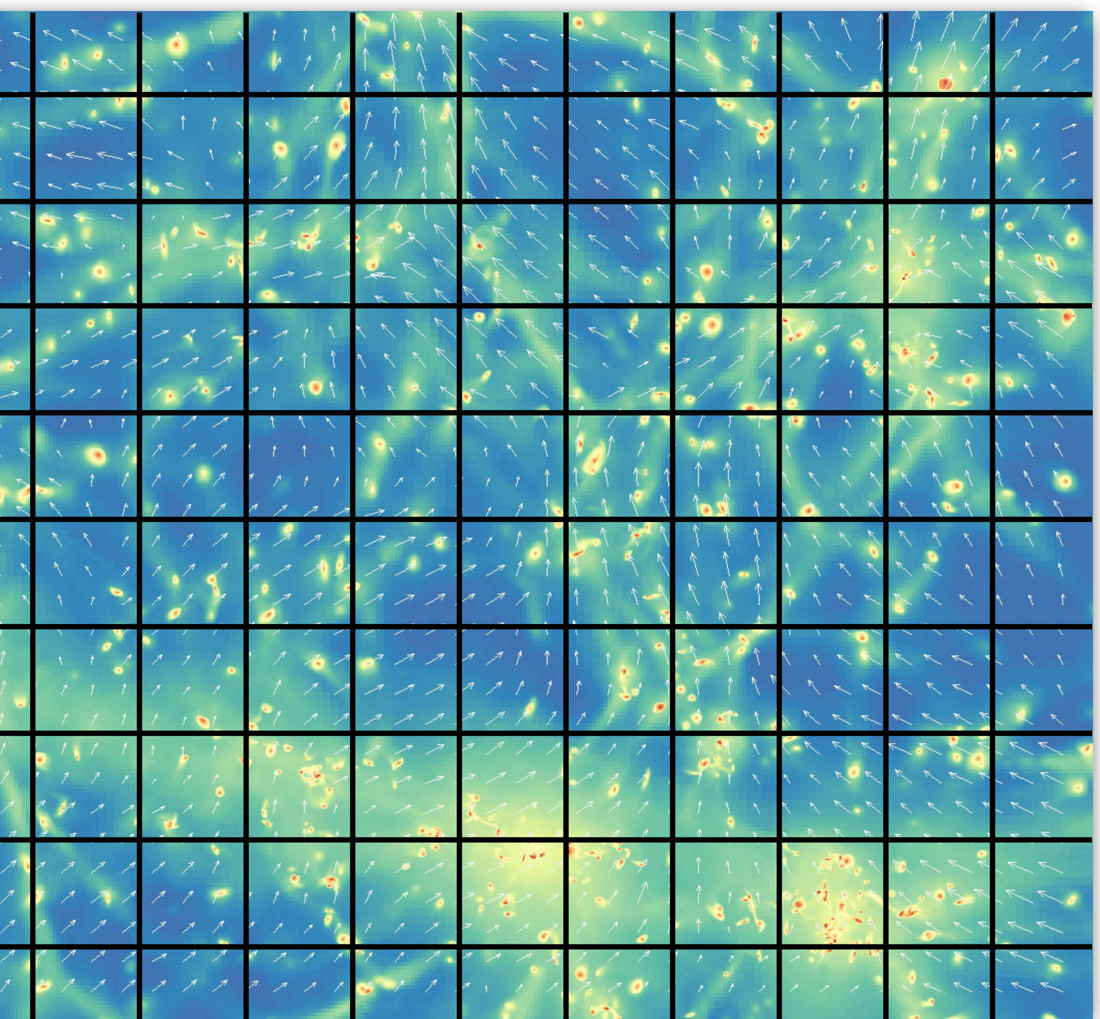

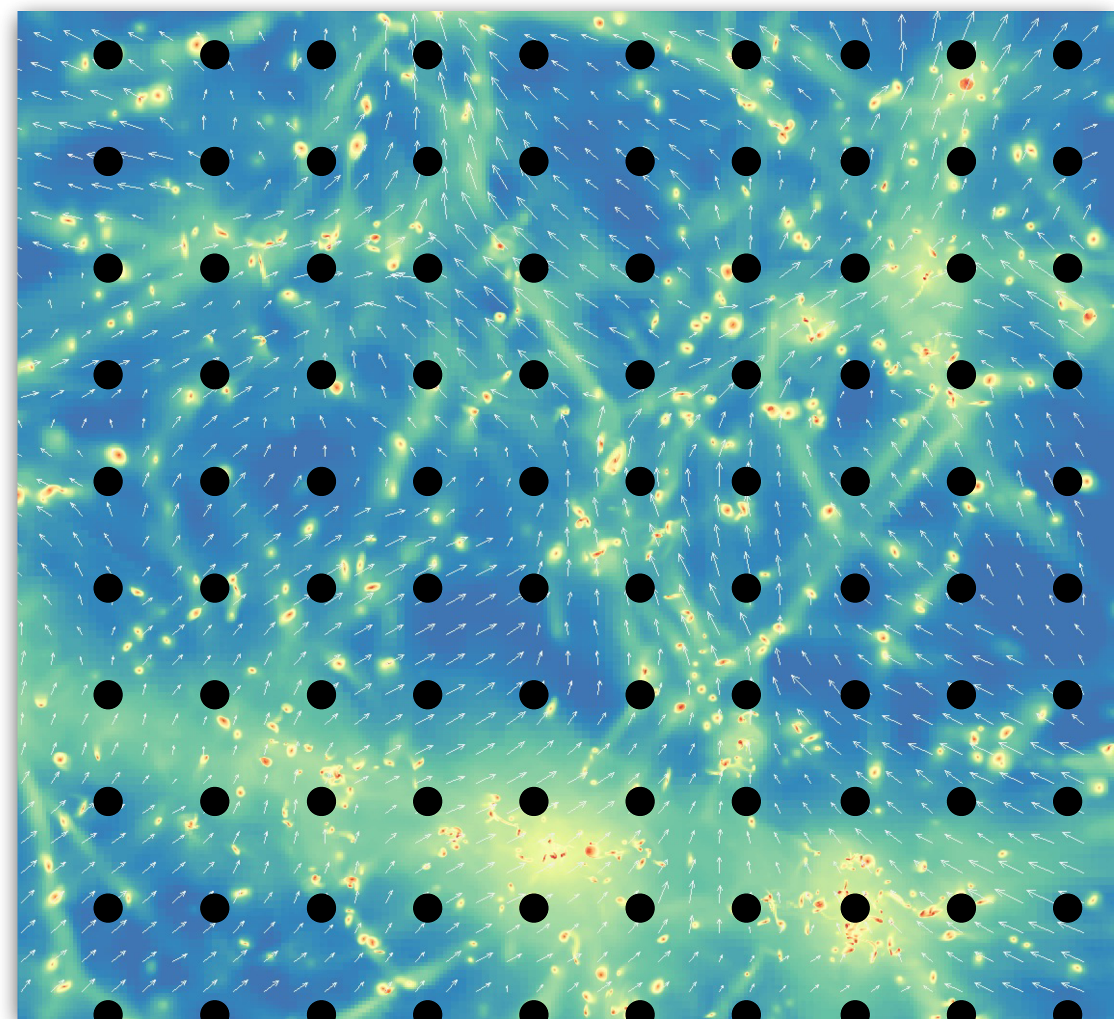

From Eulerian to Lagrangian space

Eulerian pt of view:

- Fixes the frame
- Fields on a grid
- δ, u
- « volume-weighted statistics »

Lagrangian pt of view:

- Follows the fluid
- Particules
- $x=q+\psi$
- « mass-weighted statistics »

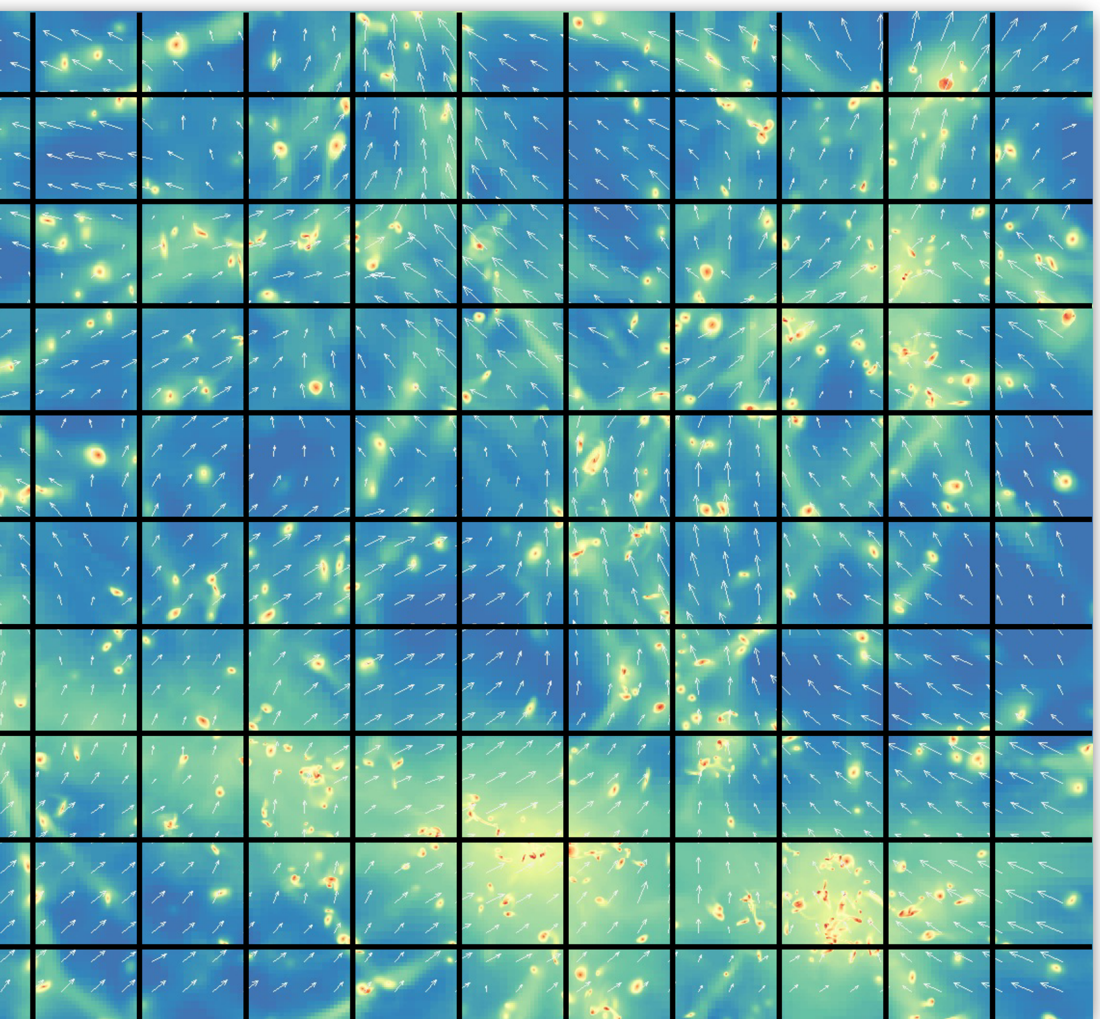

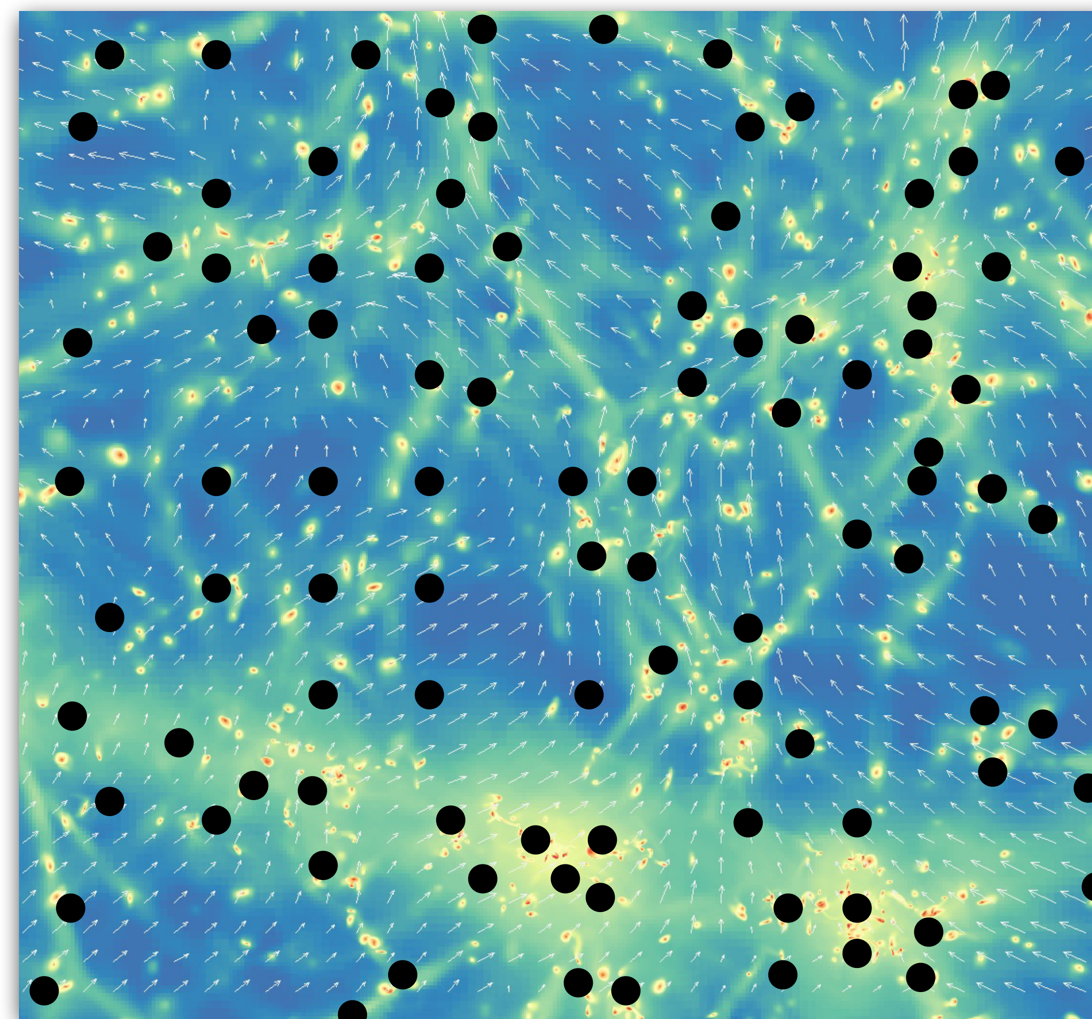

Lagrangian dynamics: Zeldovich pancakes

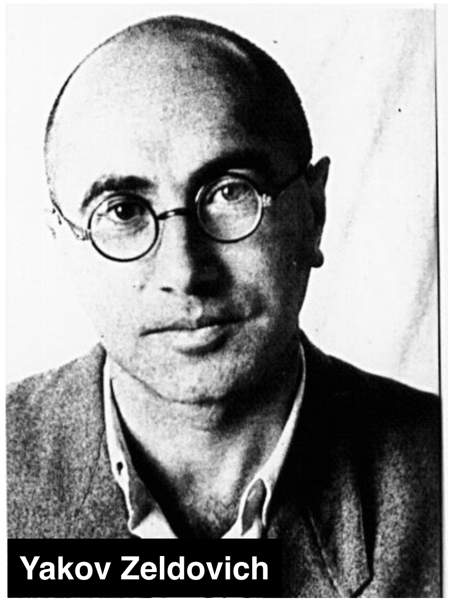

initial position

$$\mathbf{x} = \mathbf{q} + \zeta$$

final position displacement

At linear order in the displacement, the Vlasov Poisson system reduces to

$$\nabla_{\mathbf{q}}\ddot{\zeta} + 2H\nabla_{\mathbf{q}}\dot{\zeta} = \frac{3}{2}\Omega H^2 \nabla_{\mathbf{q}}\zeta$$

which has the same solution as the linear density contrast i.e

$$\zeta_{\rm ZA} = D_+(t)\zeta_+(\mathbf{q})$$

Balistic trajectories

so that the density after a Zeldovich displacement reads:

$$\boxed{\rho_{\rm ZA}(\mathbf{q}, t) = \frac{\bar{\rho}}{\left|\prod_{i=1}^{3}(1 - D_+(t)\lambda_i)\right|}}$$

eigenvalues of the deformation tensor:

$- \partial\zeta_+^{(i)}/\partial q_j$

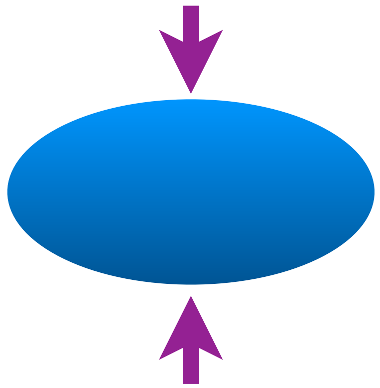

Anisotropic collapse of structures and formation of *caustics*!
Walls form first followed by filaments and nodes.

« L'essence de la théorie des catastrophes c'est de ramener les discontinuités apparentes à la manifestation d'une évolution lente sous-jacente. Le problème est alors de déterminer cette évolution lente qui, elle, exige en général l'introduction de nouvelles dimensions, de nouveaux paramètres. » - René Thom (1991)

Lagrangian dynamics: Zeldovich pancakes

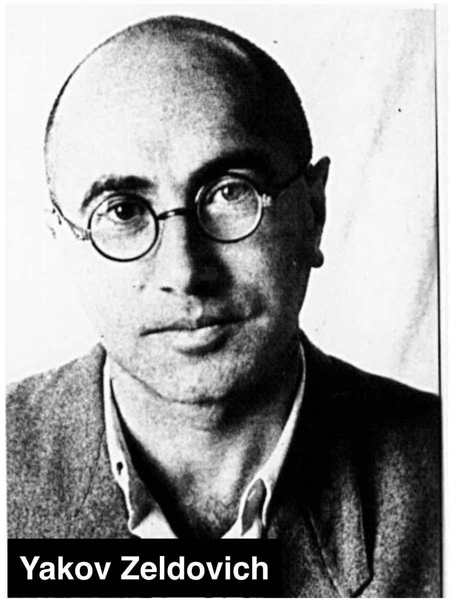

initial position

$$\mathbf{x} = \mathbf{q} + \zeta$$

final position — displacement

At linear order in the displacement, the Vlasov Poisson system reduces to

$$\nabla_{\mathbf{q}}\ddot{\zeta} + 2H\nabla_{\mathbf{q}}\dot{\zeta} = \frac{3}{2}\Omega H^2 \nabla_{\mathbf{q}}\zeta$$

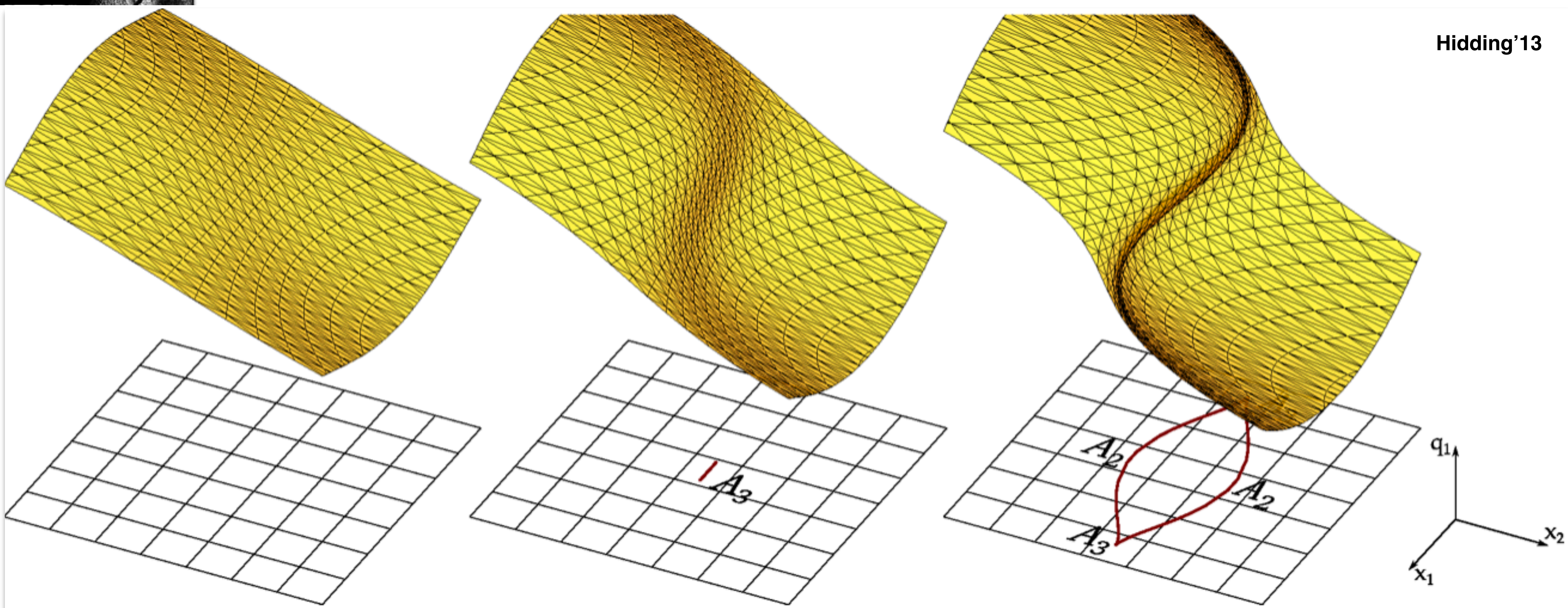

« L'essence de la théorie des catastrophes c'est de ramener les discontinuités apparentes à la manifestation d'une évolution lente sous-jacente. Le problème est alors de déterminer cette évolution lente qui, elle, exige en général l'introduction de nouvelles dimensions, de nouveaux paramètres. » - René Thom (1991)

The connected cosmic web

Bond, Kofman, Pogosyan 1996: first *understanding* of the origin of the cosmic web.

The seeds of walls, filaments and nodes lie in the asymmetries of the primordial Gaussian random field then amplified by gravitational instability.

Rare *peaks* in the ICs will become the nodes of the cosmic web i.e rich clusters. Their initial *shear* will set the preferred directions along which correlation bridges will connect them to other nodes.

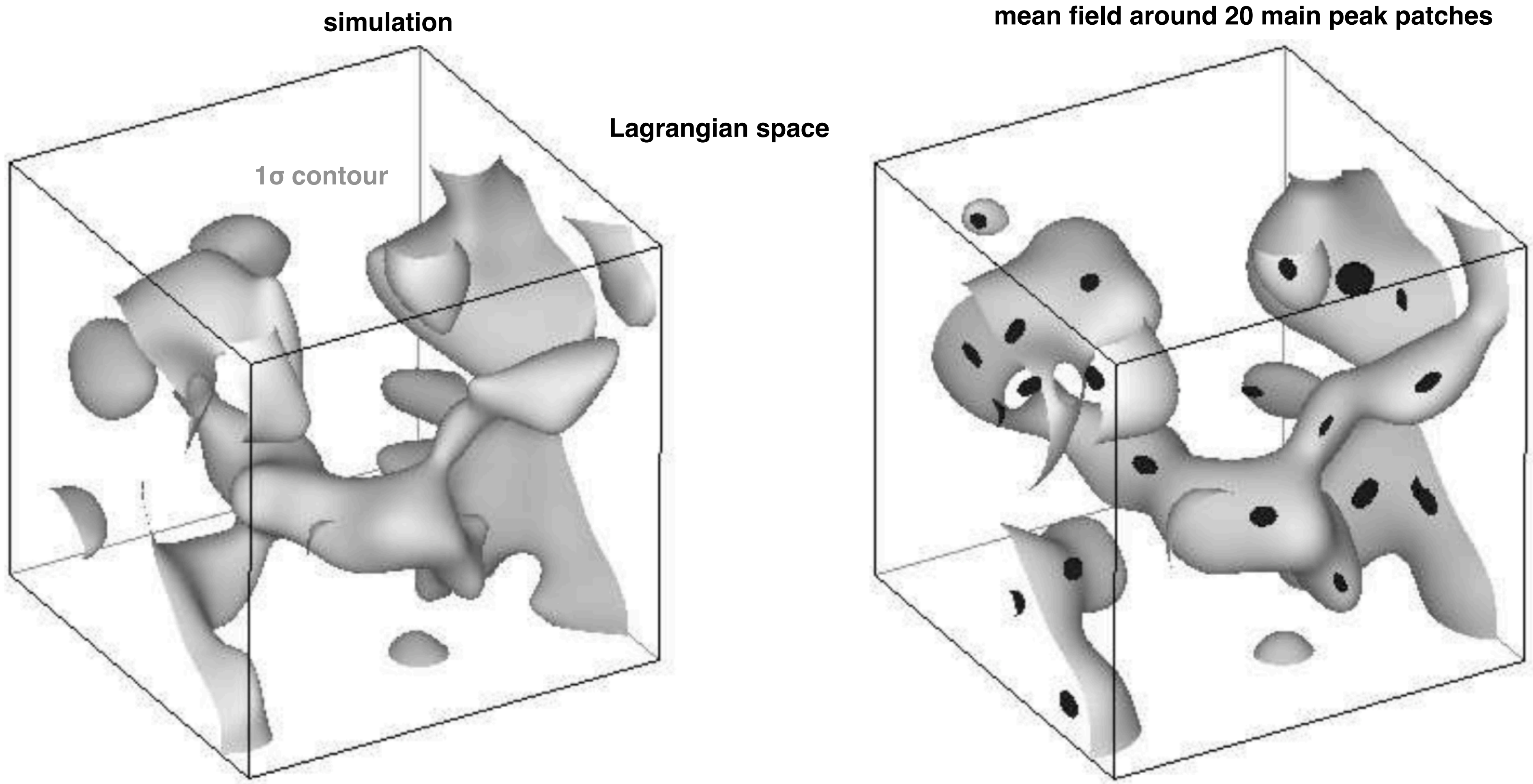

Importance of peak & constrained random field theories

The connected cosmic web

Bond, Kofman, Pogosyan 1996: first *understanding* of the origin of the cosmic web.

The seeds of walls, filaments and nodes lie in the asymmetries of the primordial Gaussian random field then amplified by gravitational instability.

Rare *peaks* in the ICs will become the nodes of the cosmic web i.e rich clusters. Their initial *shear* will set the preferred directions along which correlation bridges will connect them to other nodes.

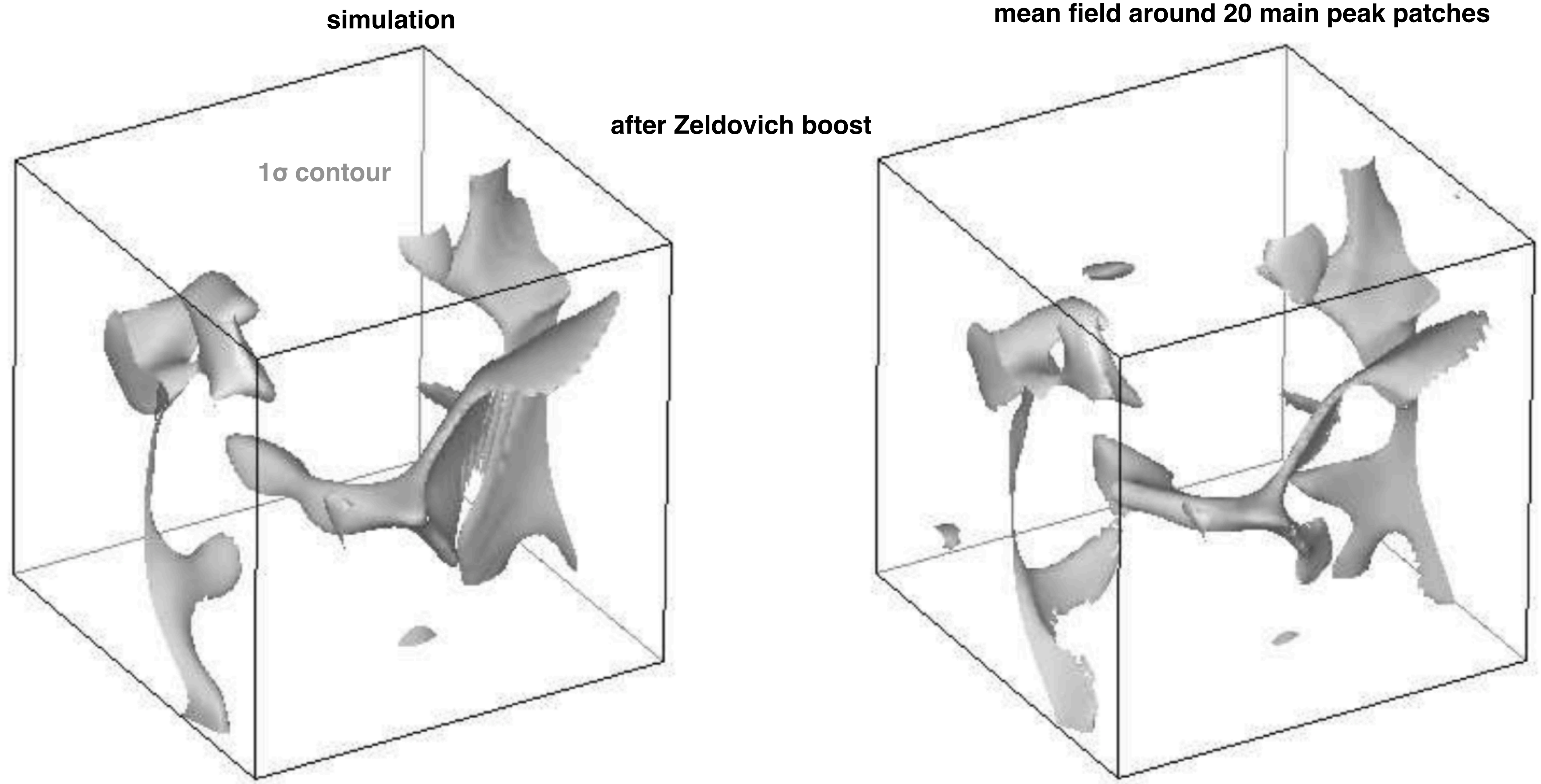

Importance of peak & constrained random field theories

The skeleton picture

Filaments are the field lines joining the maxima through saddle points.

- cosmic web extractors (water-shedding, discrete topology, …) *Sousbie+08, Sousbie+11, …**

- local theory allowing for theoretical predictions for extrema counts, length of filaments, surface of voids, curvature … which are very competitive cosmological probes! *BBKS, Pogosyan+09, Gay+12, …**

- Cosmic connectivity κ: typically, how many filaments connect to a node? *SC+18*

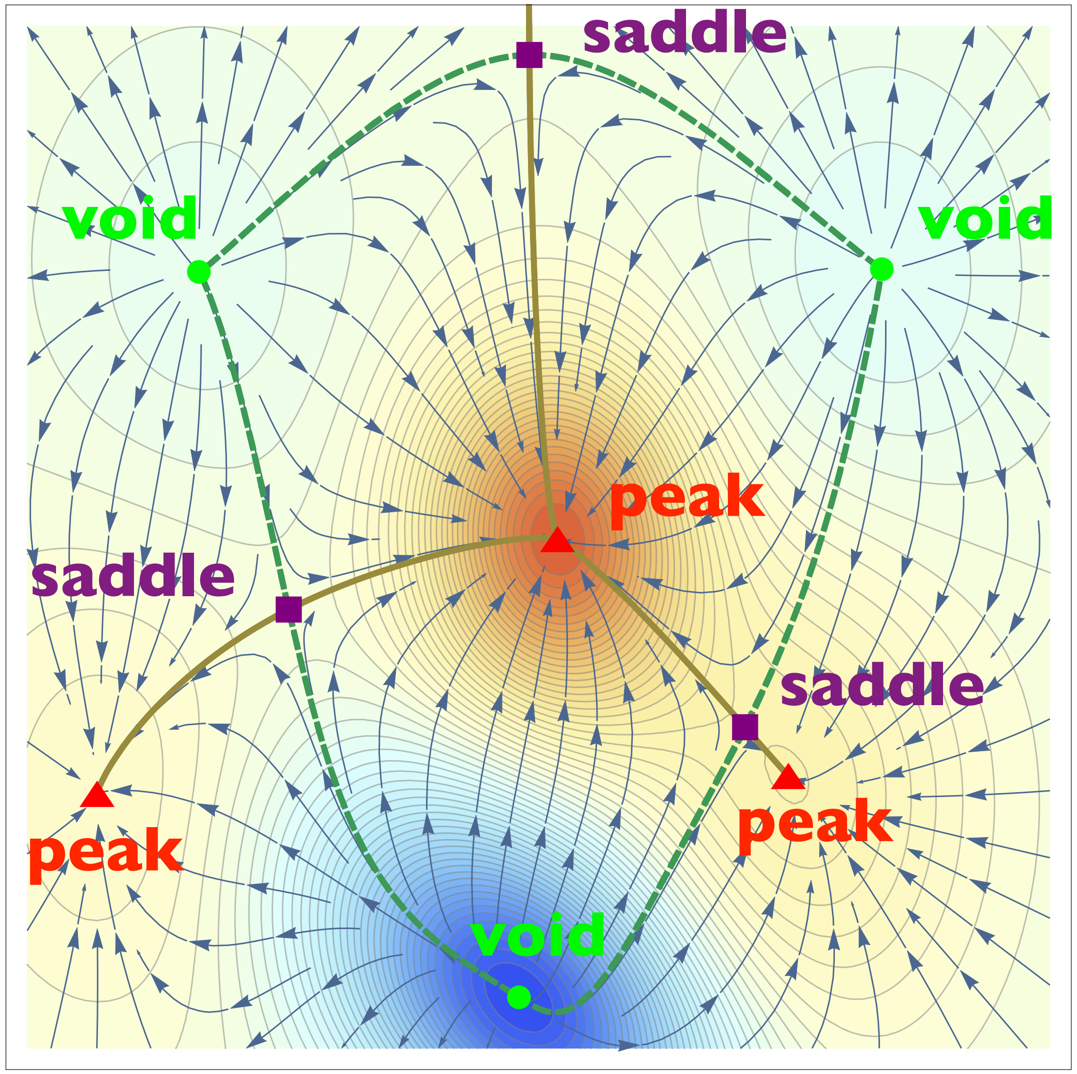

** among many others!*

The skeleton picture

Filaments are the field lines joining the maxima through saddle points.

- cosmic web extractors (water-shedding, discrete topology, …) *Sousbie+08, Sousbie+11, …**
- local theory allowing for theoretical predictions for extrema counts, length of filaments, surface of voids, curvature … which are very competitive cosmological probes! *BBKS, Pogosyan+09, Gay+12, …**
- Cosmic connectivity κ: typically, how many filaments connect to a node? *SC+18*

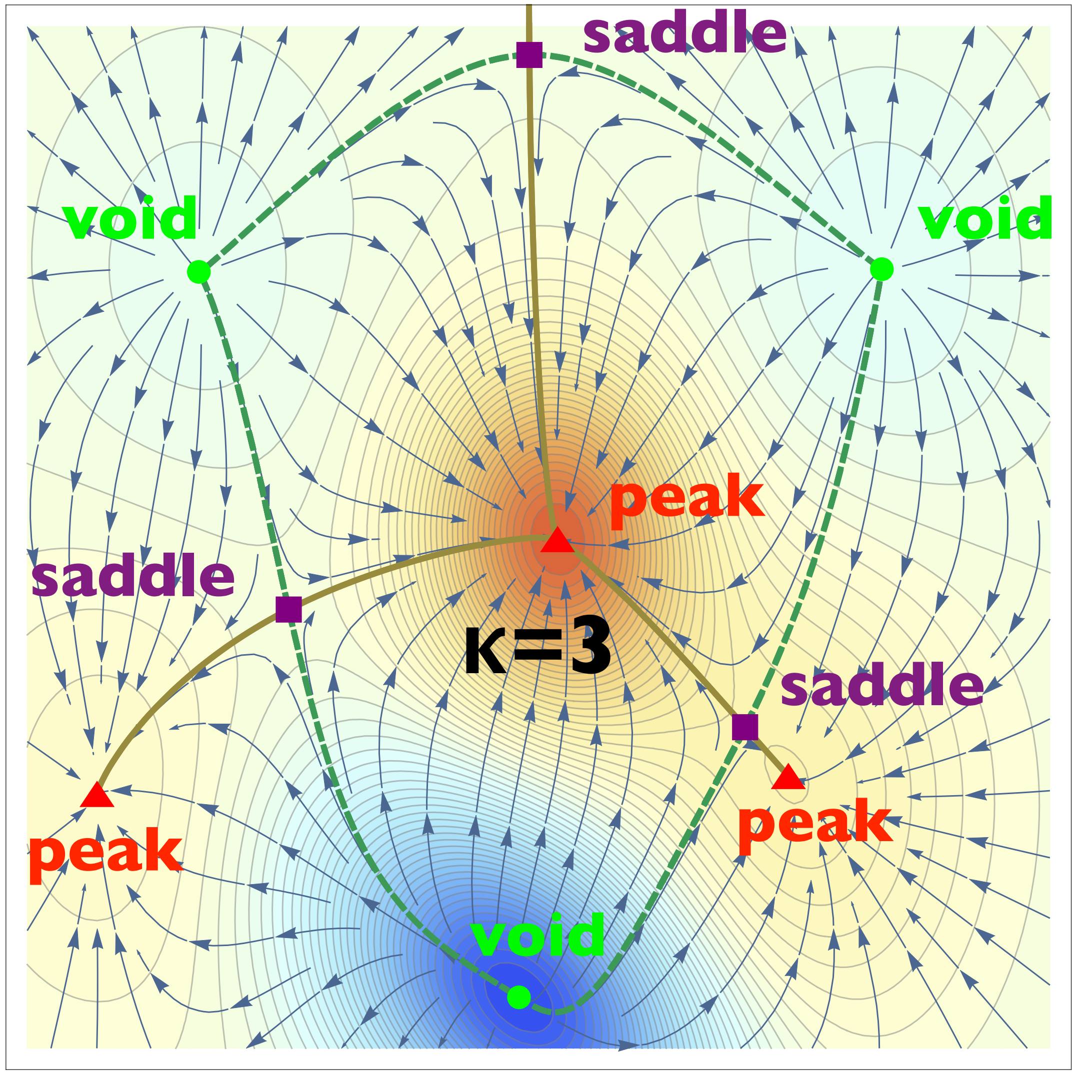

* *among many others!*

The skeleton picture

Filaments are the field lines joining the maxima through saddle points.

- cosmic web extractors (water-shedding, discrete topology, ...) *Sousbie+08, Sousbie+11, ...**

- local theory allowing for theoretical predictions for extrema counts, length of filaments, surface of voids, curvature ... which are very competitive cosmological probes! *BBKS, Pogosyan+09, Gay+12, ...**

- Cosmic connectivity κ: typically, how many filaments connect to a node? *SC+18*

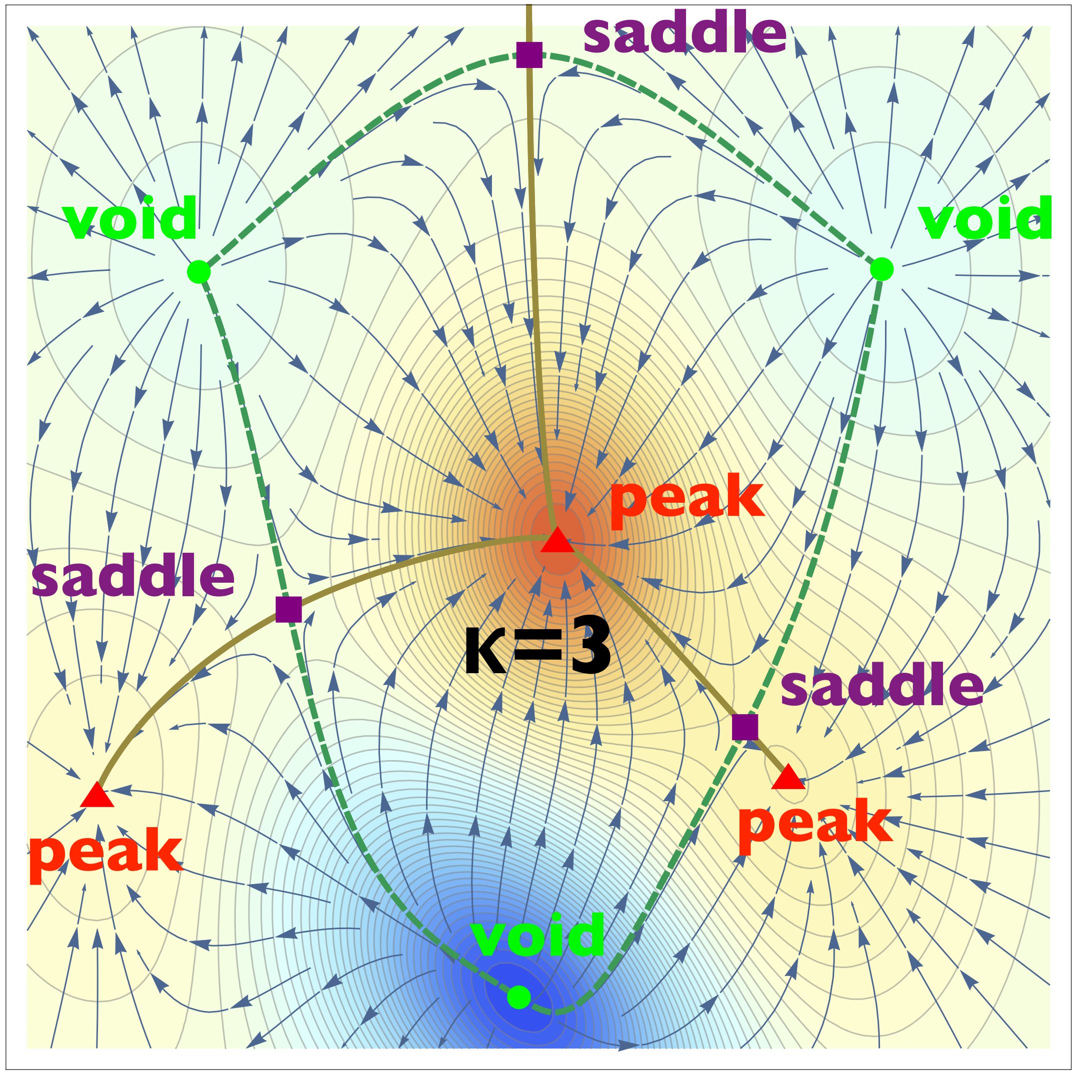

Importance of peak & constrained random field theories

* *among many others!*

On the connectivity of the cosmic web

- Birth and growth of the cosmic web
- Random fields, Peak theory, topology
- Cosmic connectivity

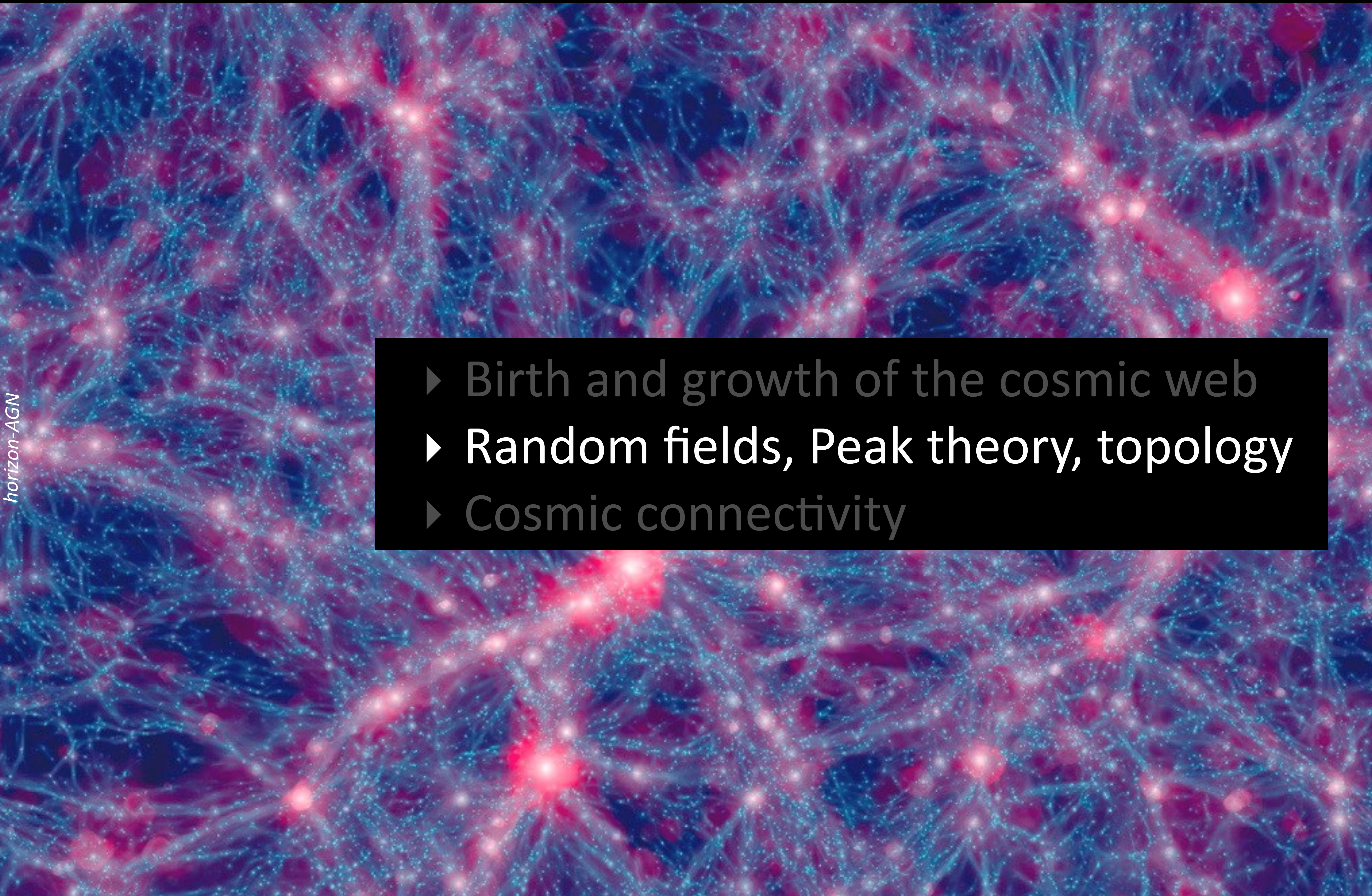

Peak theory

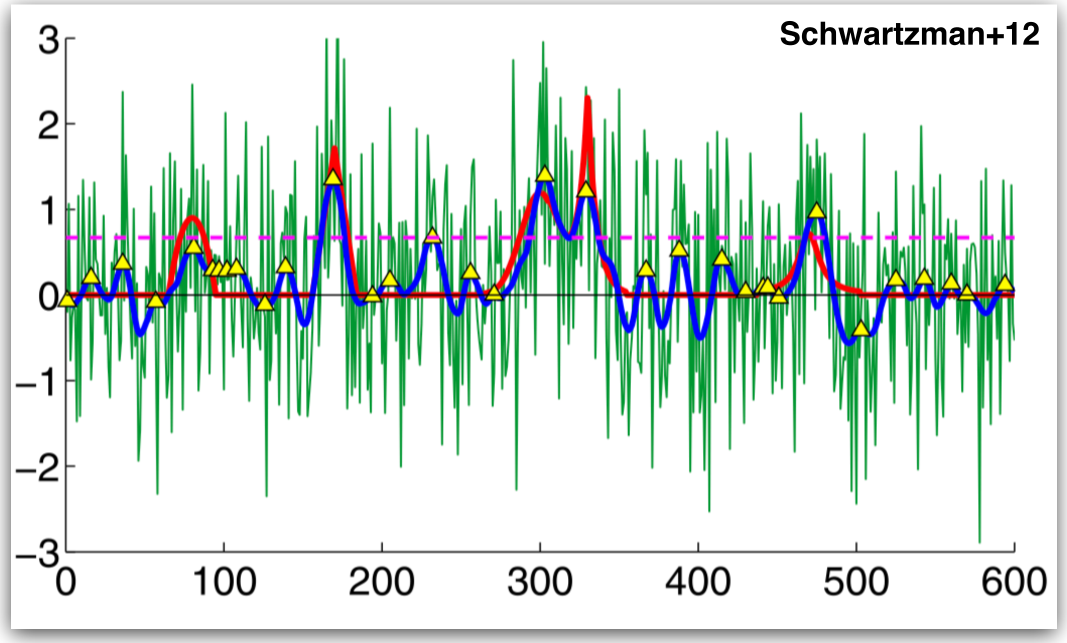

1940's: Kac-Rice first studied the peaks in 1D signals, with important applications in communication theory and electronic signals

1957: Longuet-Higgins extended this work to the 2D case in the context of ocean surface waves (width and shape of the crests, distance between troughs, …)

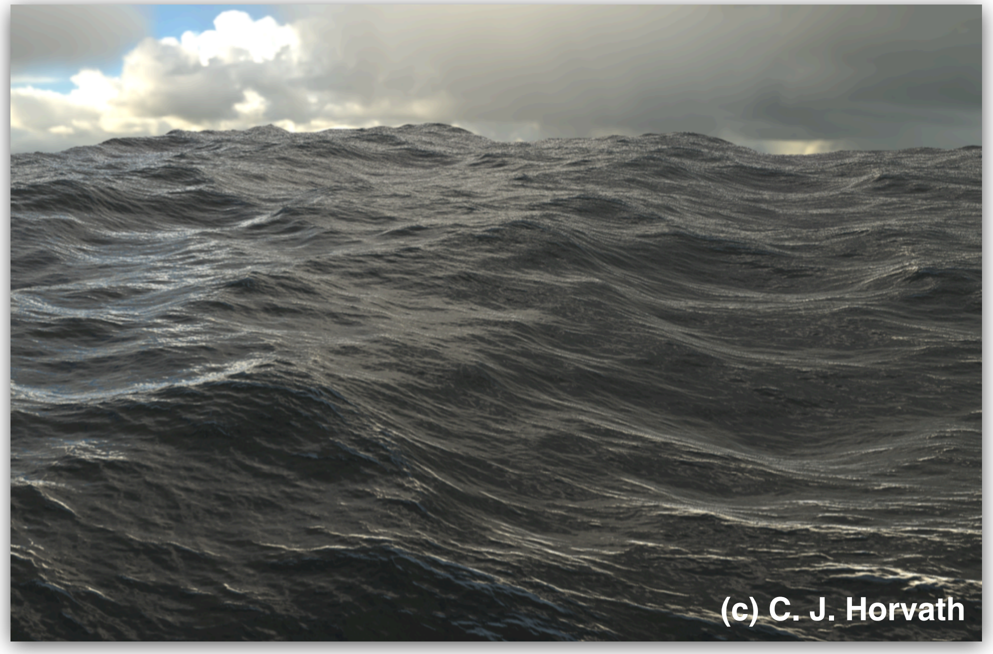

Applications to cosmology then follows with Doroshkevich (1970), Bardeen-Bond-Kaiser-Szalay (1986) and many others …

Peak theory

Let us consider a field x and its first x_i and second x_{ij} derivatives.

Peak theory

Let us consider a field x and its first x_i and second x_{ij} derivatives.

peaks = point process

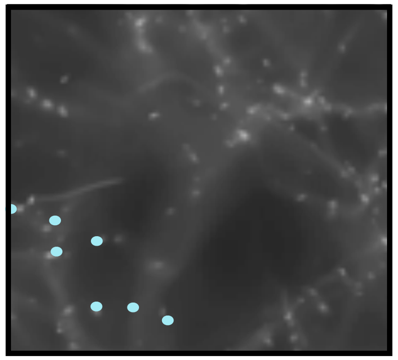

The number density of peaks is:

$$n_{\rm peak}(\vec{r}) = \sum_k \delta_D(\vec{r} - \vec{r}_{peak\ k})$$

Peak theory

Let us consider a field x and its first x_i and second x_{ij} derivatives.

peaks = point process

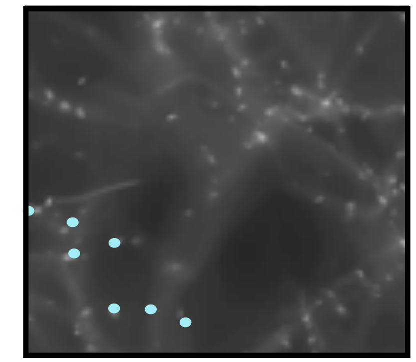

The number density of peaks is:

$$n_{\text{peak}}(\vec{r}) = \sum_k \delta_D(\vec{r} - \vec{r}_{peak\,k})$$

A Taylor expansion of x_i around a peak k reads:

$$\underset{\nabla}{x_i}(\vec{r}) = 0 + \sum_j \underset{\mathcal{H}}{x_{ij}}(\vec{r}_{\text{peak}\,k}) \times (\vec{r} - \vec{r}_{\text{peak}\,k})_j$$

Peak theory

Let us consider a field x and its first x_i and second x_{ij} derivatives.

peaks = point process

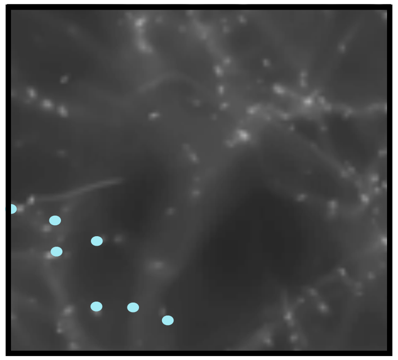

The number density of peaks is:

$$n_{\text{peak}}(\vec{r}) = \sum_k \delta_D(\vec{r} - \vec{r}_{peak\,k})$$

A Taylor expansion of x_i around a peak k reads:

$$\underset{\nabla}{x_i}(\vec{r}) = 0 + \sum_j \underset{\mathcal{H}}{x_{ij}}(\vec{r}_{\text{peak}\,k}) \times (\vec{r} - \vec{r}_{\text{peak}\,k})_j$$

which can be inverted : $(\vec{r} - \vec{r}_{\text{peak}\,k}) = \mathcal{H}^{-1}(\vec{r}_{\text{peak}\,k}) \cdot \nabla(\vec{r})$

Peak theory

Let us consider a field x and its first x_i and second x_{ij} derivatives.

peaks = point process

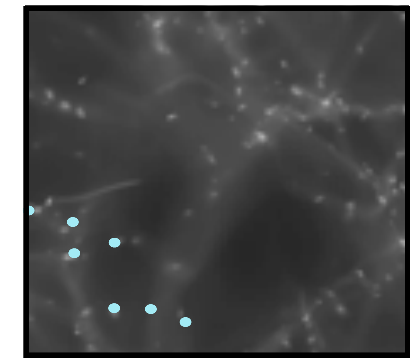

The number density of peaks is:

$$n_{\rm peak}(\vec{r}) = \sum_k \delta_D(\vec{r} - \vec{r}_{peak\,k})$$

A Taylor expansion of x_i around a peak k reads:

$$\underset{\nabla}{x_i}(\vec{r}) = 0 + \sum_j \underset{\mathcal{H}}{x_{ij}}(\vec{r}_{\rm peak\,\mathit{k}}) \times (\vec{r} - \vec{r}_{\rm peak\,\mathit{k}})_j$$

which can be inverted : $(\vec{r} - \vec{r}_{\rm peak\,\mathit{k}}) = \mathcal{H}^{-1}(\vec{r}_{\rm peak\,\mathit{k}}) \cdot \nabla(\vec{r})$

So that in the end:

$$\langle n_{\rm peak} \rangle = \int \frac{{\rm d}^3\vec{r}}{V}\, n_{\rm peak}(\vec{r}) = \int {\rm d}x\, {\rm d}^3 x_i\, {\rm d}^6 x_{ij} P(x, x_i, x_{ij}) |\det x_{ij}| \delta_D(x_i)$$

Peak theory

Let us consider a field x and its first x_i and second x_{ij} derivatives.

peaks = point process

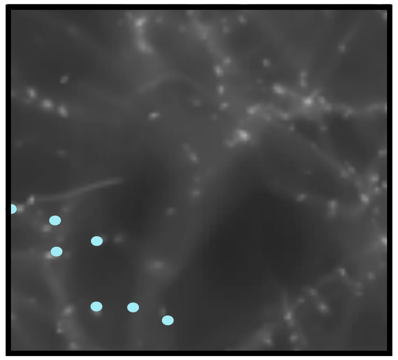

The number density of peaks is:

$$n_{\rm peak}(\vec{r}) = \sum_k \delta_D(\vec{r} - \vec{r}_{{\rm peak}\,k})$$

A Taylor expansion of x_i around a peak k reads:

$$\underset{\nabla}{x_i}(\vec{r}) = 0 + \sum_j \underset{\mathcal{H}}{x_{ij}}(\vec{r}_{{\rm peak}\,k}) \times (\vec{r} - \vec{r}_{{\rm peak}\,k})_j$$

which can be inverted : $(\vec{r} - \vec{r}_{{\rm peak}\,k}) = \mathcal{H}^{-1}(\vec{r}_{{\rm peak}\,k}) \cdot \nabla(\vec{r})$

So that in the end:

$$\langle n_{\rm peak} \rangle = \int \frac{{\rm d}^3\vec{r}}{V}\, n_{\rm peak}(\vec{r}) = \int {\rm d}x\, {\rm d}^3x_i\, {\rm d}^6x_{ij} P(x, x_i, x_{ij}) |\det x_{ij}| \delta_D(x_i)$$

ergodicity!

spatial average=ensemble average

Peak theory

Let us consider a field x and its first x_i and second x_{ij} derivatives.

peaks = point process

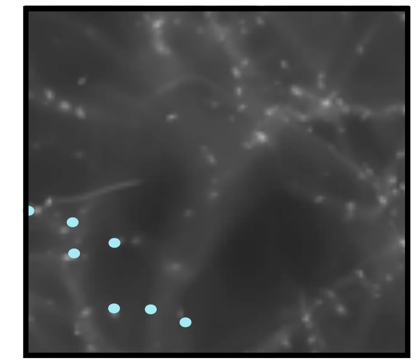

The number density of peaks is:

$$n_{\rm peak}(\vec r) = \sum_k \delta_D(\vec r - \vec r_{{\rm peak}\,k})$$

A Taylor expansion of x_i around a peak k reads:

$$x_i(\vec r) = 0 + \sum_j x_{ij}(\vec r_{{\rm peak}\,k}) \times (\vec r - \vec r_{{\rm peak}\,k})_j$$

∇ $\mathcal{H}$

which can be inverted : $(\vec r - \vec r_{{\rm peak}\,k}) = \mathcal{H}^{-1}(\vec r_{{\rm peak}\,k}) \cdot \nabla(\vec r)$

So that in the end:

$$\langle n_{\rm peak}\rangle = \int \frac{{\rm d}^3\vec r}{V}\, n_{\rm peak}(\vec r) = \int {\rm d}x\, {\rm d}^3x_i\, {\rm d}^6x_{ij} P(x, x_i, x_{ij})|\det x_{ij}|\delta_D(x_i) \times\Theta(-\lambda_1)$$

ergodicity!

spatial average=ensemble average

Peak theory

Let us consider a field x and its first x_i and second x_{ij} derivatives.

peaks = point process

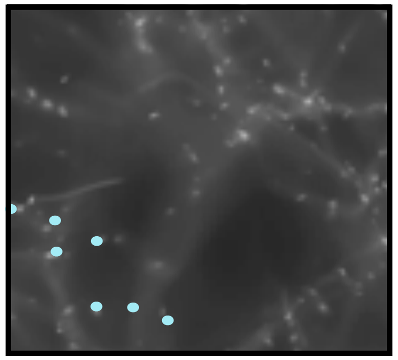

The number density of peaks is:

$$n_{\rm peak}(\vec r) = \sum_k \delta_D(\vec r - \vec r_{peak\,k})$$

A Taylor expansion of x_i around a peak k reads:

$$x_i(\vec r) = 0 + \sum_j x_{ij}(\vec r_{{\rm peak}\,k}) \times (\vec r - \vec r_{{\rm peak}\,k})_j$$

∇ $\mathcal{H}$

which can be inverted : $(\vec r - \vec r_{{\rm peak}\,k}) = \mathcal{H}^{-1}(\vec r_{{\rm peak}\,k}) \cdot \nabla(\vec r)$

So that in the end:

$$\langle n_{\rm peak}\rangle(\nu) = \int \frac{{\rm d}^3 \vec r}{V}\, n_{\rm peak}(\vec r) = \int {\rm d}x\, {\rm d}^3 x_i\, {\rm d}^6 x_{ij} P(x, x_i, x_{ij}) |\det x_{ij}| \delta_D(x_i) \times \Theta(-\lambda_1) \times \Theta(x - \sigma_0 \nu)$$

ergodicity!

spatial average=ensemble average

Peak theory

Let us consider a field x and its first x_i and second x_{ij} derivatives.

peaks = point process

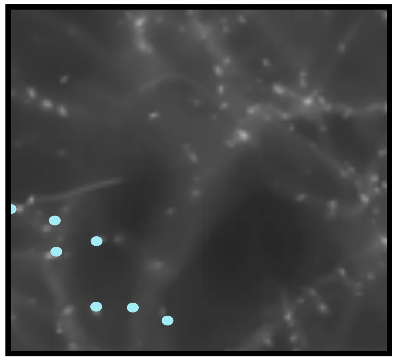

The number density of peaks is:

$$n_{\rm peak}(\vec r) = \sum_k \delta_D(\vec r - \vec r_{peak\,k})$$

A Taylor expansion of x_i around a peak k reads:

$$\underset{\nabla}{x_i}(\vec r) = 0 + \sum_j \underset{\mathcal{H}}{x_{ij}}(\vec r_{{\rm peak}\,k}) \times (\vec r - \vec r_{{\rm peak}\,k})_j$$

which can be inverted : $(\vec r - \vec r_{{\rm peak}\,k}) = \mathcal{H}^{-1}(\vec r_{{\rm peak}\,k}) \cdot \nabla(\vec r)$

So that in the end:

$$\langle n_{\rm peak}\rangle (\nu) = \int \frac{{\rm d}^3 \vec r}{V} n_{\rm peak}(\vec r) = \int {\rm d}x\, {\rm d}^3 x_i\, {\rm d}^6 x_{ij}\, P(x, x_i, x_{ij}) |\det x_{ij}| \delta_D(x_i) \times \Theta(-\lambda_1) \times \Theta(x - \sigma_0 \nu)$$

ergodicity!
spatial average=ensemble average

Peak theory: Gaussian predictions

If the field is Gaussian (large scales/early times), $X = (x, x_i, x_{ij})$ follows a normal distribution

$$P(x, x_i, x_{ij}) = \frac{\mathrm{Exp}\left(-\frac{X^t \cdot C^{-1} \cdot X}{2}\right)}{\sqrt{\det(2\pi C)}}$$

where the covariance matrix C of the field, its first and second derivatives can easily be computed from the power spectrum.
E.g in 3D, once the fields are rescaled by their variance:

$$C = \begin{array}{c} \begin{array}{cccccccccc} x & x_1 & x_2 & x_3 & x_{11} & \cdots & & & & \end{array} \\ \begin{pmatrix} 1 & 0 & 0 & 0 & -\gamma/3 & -\gamma/3 & -\gamma/3 & 0 & 0 & 0 \\ 0 & 1/3 & 0 & 0 & 0 & 0 & 0 & 0 & 0 & 0 \\ 0 & 0 & 1/3 & 0 & 0 & 0 & 0 & 0 & 0 & 0 \\ 0 & 0 & 0 & 1/3 & 0 & 0 & 0 & 0 & 0 & 0 \\ -\gamma/3 & 0 & 0 & 0 & 1/5 & 1/15 & 1/15 & 0 & 0 & 0 \\ -\gamma/3 & 0 & 0 & 0 & 1/15 & 1/5 & 1/15 & 0 & 0 & 0 \\ -\gamma/3 & 0 & 0 & 0 & 1/15 & 1/15 & 1/5 & 0 & 0 & 0 \\ 0 & 0 & 0 & 0 & 0 & 0 & 0 & 1/15 & 0 & 0 \\ 0 & 0 & 0 & 0 & 0 & 0 & 0 & 0 & 1/15 & 0 \\ 0 & 0 & 0 & 0 & 0 & 0 & 0 & 0 & 0 & 1/15 \end{pmatrix} \end{array}$$

with spectral parameter

$$\gamma = \frac{\sigma_1^2}{\sigma_0 \sigma_2} = \frac{\langle \nabla x^2 \rangle}{\sqrt{\langle x^2 \rangle \langle \Delta x^2 \rangle}}$$

Peak theory: Gaussian predictions

If the field is Gaussian (large scales/early times), the total number density of critical points then reads

2D

$$\langle n_{\rm max}\rangle = \langle n_{\rm min}\rangle = \frac{1}{8\sqrt{3}\pi R_\star^2}$$
$$\langle n_{\rm sad}\rangle = \frac{1}{4\sqrt{3}\pi R_\star^2}$$

3D

$$\langle n_{\rm max}\rangle = \langle n_{\rm min}\rangle = \frac{29\sqrt{15} - 18\sqrt{10}}{1800\pi^2 R_\star^3}$$
$$\langle n_{\rm sadf}\rangle = \langle n_{\rm sadw}\rangle = \frac{29\sqrt{15} + 18\sqrt{10}}{1800\pi^2 R_\star^3},$$

Peak theory: Gaussian predictions

If the field is Gaussian (large scales/early times), the total number density of critical points then reads

2D

$$\langle n_{\rm max}\rangle = \langle n_{\rm min}\rangle = \frac{1}{8\sqrt{3}\pi R_\star^2}$$

$$\langle n_{\rm sad}\rangle = \frac{1}{4\sqrt{3}\pi R_\star^2}$$

3D

$$\langle n_{\rm max}\rangle = \langle n_{\rm min}\rangle = \frac{29\sqrt{15}-18\sqrt{10}}{1800\pi^2 R_\star^3}$$

$$\langle n_{\rm sadf}\rangle = \langle n_{\rm sadw}\rangle = \frac{29\sqrt{15}+18\sqrt{10}}{1800\pi^2 R_\star^3},$$

And as a function of peak height (analytical in 2D, not in 3D) :

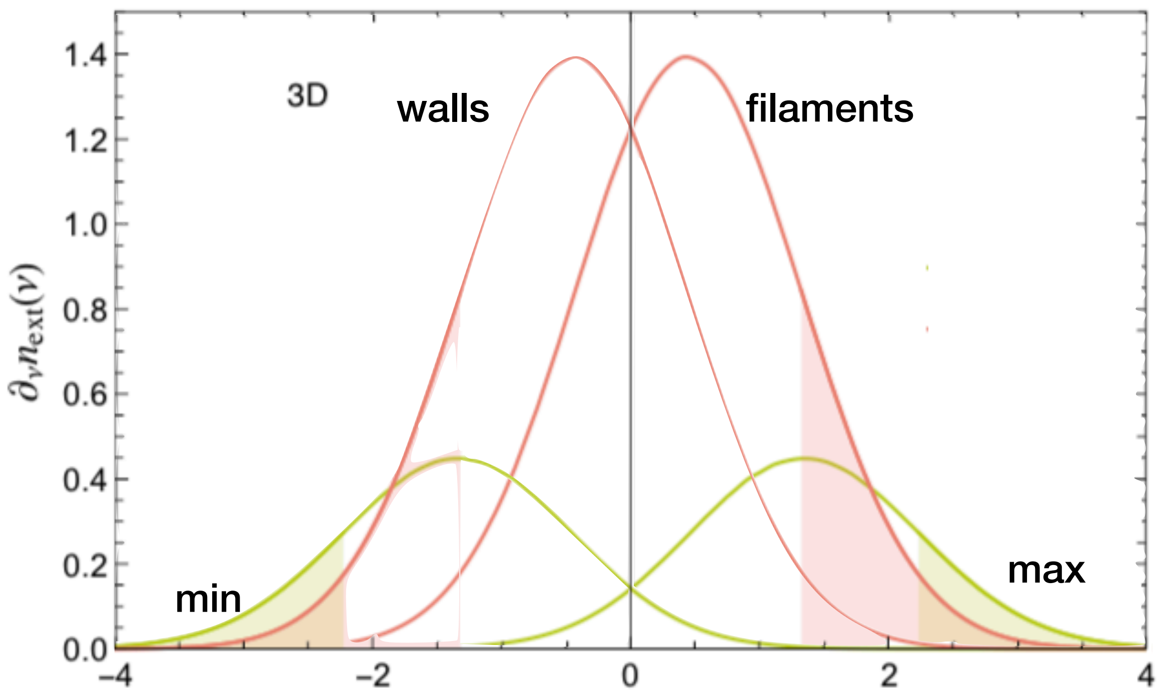

Peak theory: Non-Gaussian predictions

Gay+11

see also Pogosyan+00, Gay+11, SC+13

Gram-Charlier expansion (analogous to a Taylor expansion for PDF)***:***
The moment expansion of the general PDF P(x) around a Gaussian G(x) is an Hermite expansion:

$$P(x) = G(x)\left[1 + \sum_{n=3}^{\infty} \frac{1}{n!} \langle x^n \rangle_{GC} H_n(x)\right]$$

to all order in non gaussianity

where Hermite polynomials are polynomials of order n in x, orthogonal wrt the Gaussian kernel G.

A similar expansion holds for $P(x, x_i, x_{ij})$

Peak theory: Non-Gaussian predictions

see also Pogosyan+00, Gay+11, SC+13

Gram-Charlier expansion (analogous to a Taylor expansion for PDF)***:***
The moment expansion of the general PDF P(x) around a Gaussian G(x) is an Hermite expansion:

$$P(x) = G(x)\left[1 + \sum_{n=3}^{\infty} \frac{1}{n!} \left\langle x^n \right\rangle_{GC} H_n(x)\right]$$

to all order in non gaussianity

where Hermite polynomials are polynomials of order n in x, orthogonal wrt the Gaussian kernel G.

A similar expansion holds for $P(x, x_i, x_{ij})$
and allows us to get predictions for number density of peaks to all order in non-Gaussianity once rotational invariants are used :

$$\begin{aligned}
n_{\mp--} &= \frac{29\sqrt{15} \mp 18\sqrt{10}}{1800\pi^2 R_*^3} + \frac{5\sqrt{5}}{24\pi^2\sqrt{6\pi}R_*^3}\left(\left\langle q^2 J_1\right\rangle - \frac{8}{21}\left\langle {J_1}^3\right\rangle + \frac{10}{21}\left\langle J_1 J_2\right\rangle\right) \\
n_{++\pm} &= \frac{29\sqrt{15} \mp 18\sqrt{10}}{1800\pi^2 R_*^3} - \frac{5\sqrt{5}}{24\pi^2\sqrt{6\pi}R_*^3}\left(\left\langle q^2 J_1\right\rangle - \frac{8}{21}\left\langle {J_1}^3\right\rangle + \frac{10}{21}\left\langle J_1 J_2\right\rangle\right)
\end{aligned}$$

Peak theory: Non-Gaussian predictions

Gay+11

see also Pogosyan+00, Gay+11, SC+13

Gram-Charlier expansion (analogous to a Taylor expansion for PDF)***:***
The moment expansion of the general PDF P(x) around a Gaussian G(x) is an Hermite expansion:

$$P(x) = G(x)\left[1 + \sum_{n=3}^{\infty} \frac{1}{n!} \langle x^n \rangle_{GC} H_n(x)\right]$$

to all order in non gaussianity

where Hermite polynomials are polynomials of order n in x, orthogonal wrt the Gaussian kernel G.

A similar expansion holds for $P(x, x_i, x_{ij})$

and allows us to get predictions for number density of peaks to all order in non-Gaussianity once rotational invariants are used :

$$n_{\mp--} = \frac{29\sqrt{15} \mp 18\sqrt{10}}{1800\pi^2 R_*^3} + \frac{5\sqrt{5}}{24\pi^2\sqrt{6\pi} R_*^3}\left(\langle q^2 J_1 \rangle - \frac{8}{21}\langle {J_1}^3 \rangle + \frac{10}{21}\langle J_1 J_2 \rangle\right)$$

$$n_{++\pm} = \frac{29\sqrt{15} \mp 18\sqrt{10}}{1800\pi^2 R_*^3} - \frac{5\sqrt{5}}{24\pi^2\sqrt{6\pi} R_*^3}\left(\langle q^2 J_1 \rangle - \frac{8}{21}\langle {J_1}^3 \rangle + \frac{10}{21}\langle J_1 J_2 \rangle\right)$$

Those cumulants can be predicted from PT $\propto \sigma$

Peak theory: Non-Gaussian predictions

...an+00, Gay+11, SC+13

Gram...

The n... ...ermite

expan...

...on gaussianity

wher... ...he

Gaus...

A sim...

and a... ...n-

Gaus...

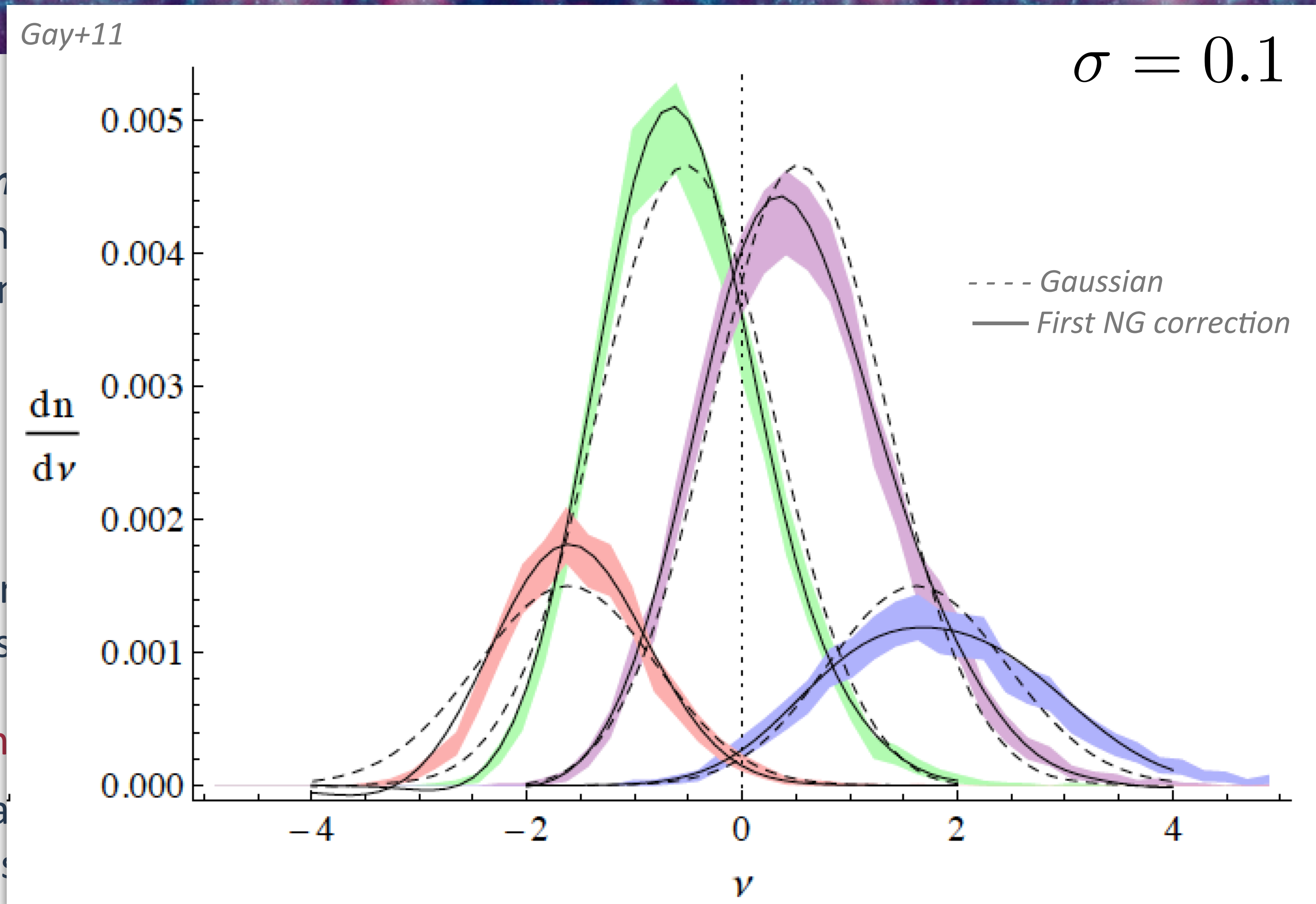

$$n_{\mp--} = \frac{29\sqrt{15} \mp 18\sqrt{10}}{1800\pi^2 R_*^3} + \frac{5\sqrt{5}}{24\pi^2\sqrt{6\pi}R_*^3}\left(\langle q^2 J_1\rangle - \frac{8}{21}\langle {J_1}^3\rangle + \frac{10}{21}\langle J_1 J_2\rangle\right)$$

$$n_{++\pm} = \frac{29\sqrt{15} \mp 18\sqrt{10}}{1800\pi^2 R_*^3} - \frac{5\sqrt{5}}{24\pi^2\sqrt{6\pi}R_*^3}\left(\langle q^2 J_1\rangle - \frac{8}{21}\langle {J_1}^3\rangle + \frac{10}{21}\langle J_1 J_2\rangle\right)$$

Those cumulants can be predicted from PT $\propto \sigma$

Peak theory: clustering (i.e 2pt stat)

Same ideas can be used to also predict the clustering of peaks by means of their 2 point correlation function (higher order statistics are also possible although not much investigated so far):

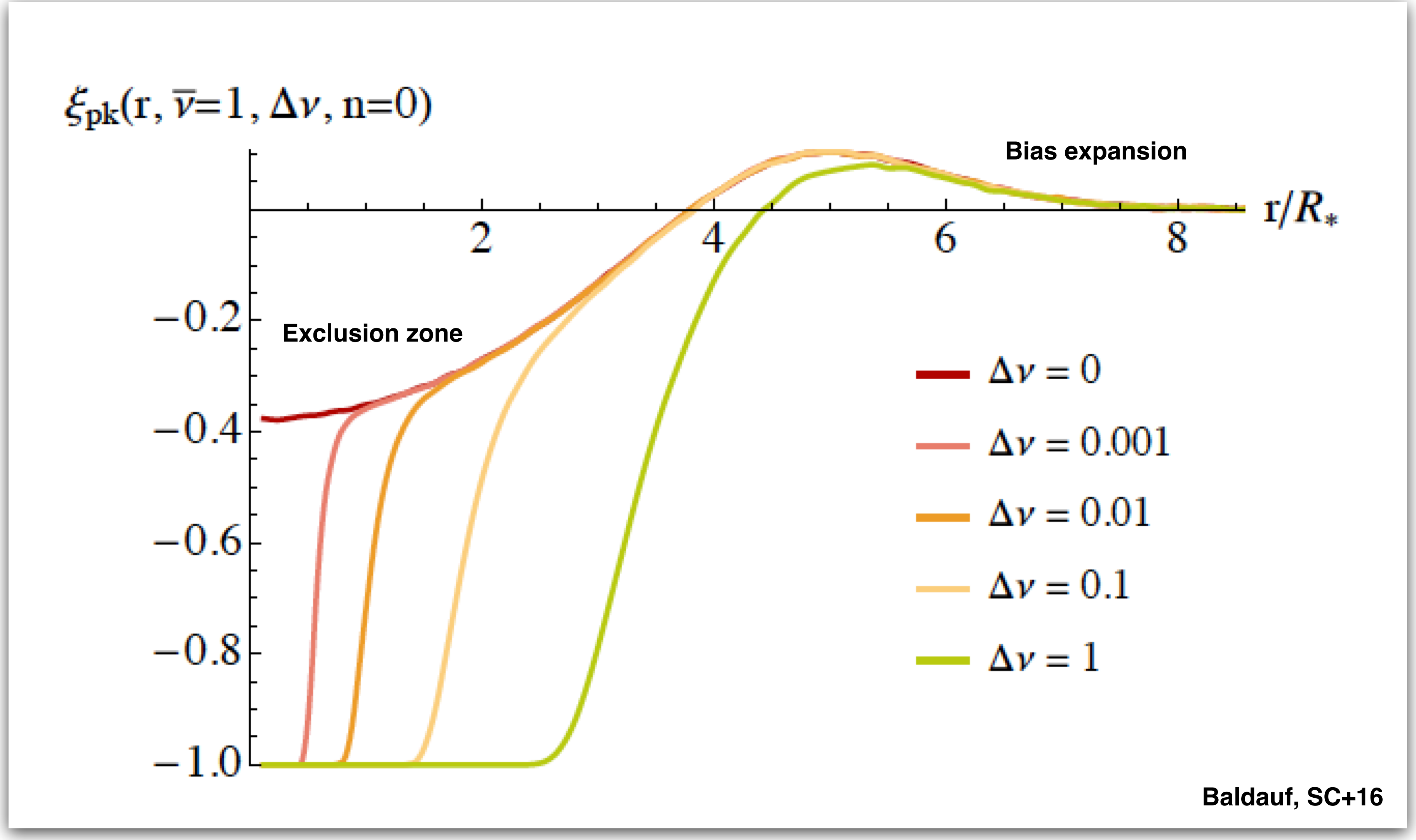

Topological estimators

Alternative to the usual use of N-point correlation functions / poly-spectra,... which is :

- independent from bias (M/L ratio)
- easier to measure in the data (less sensitive to masks,...), more robust

Because topology is about shapes, connectivity, holes,... and is ***invariant*** under ***continuous*** deformation (stretching, twisting, bending...).

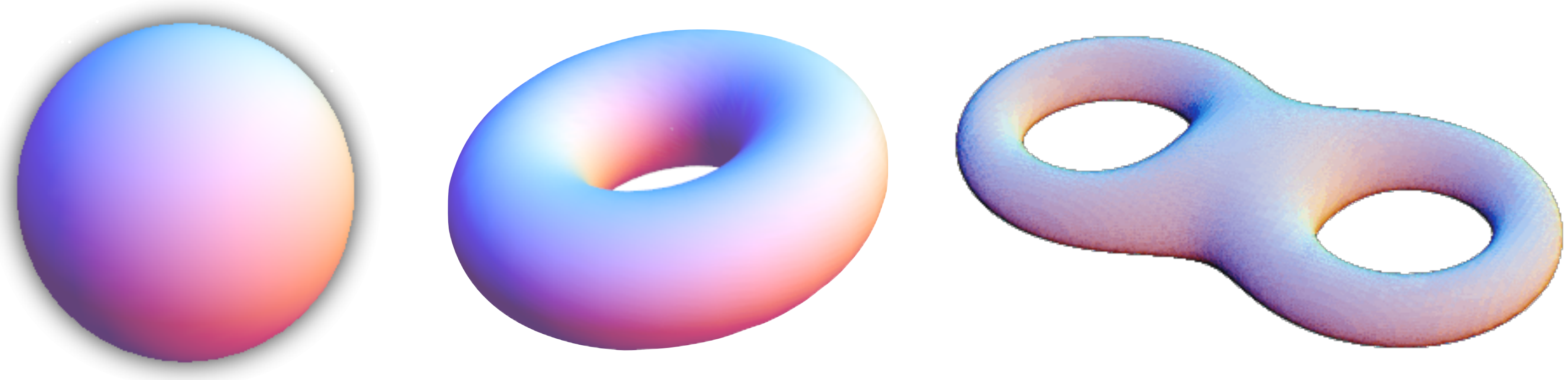

Topology of excursion sets

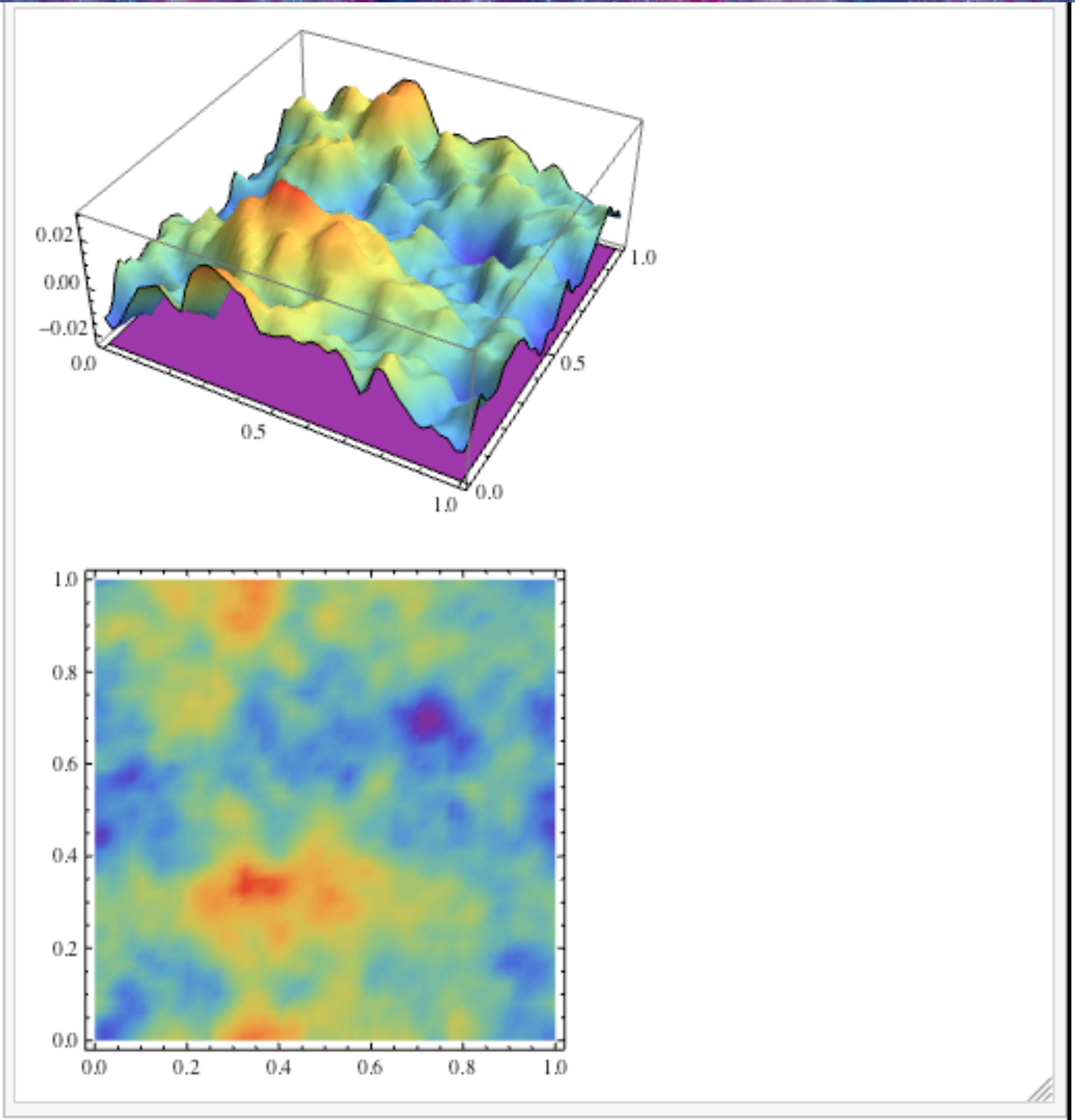

Topology of excursion sets

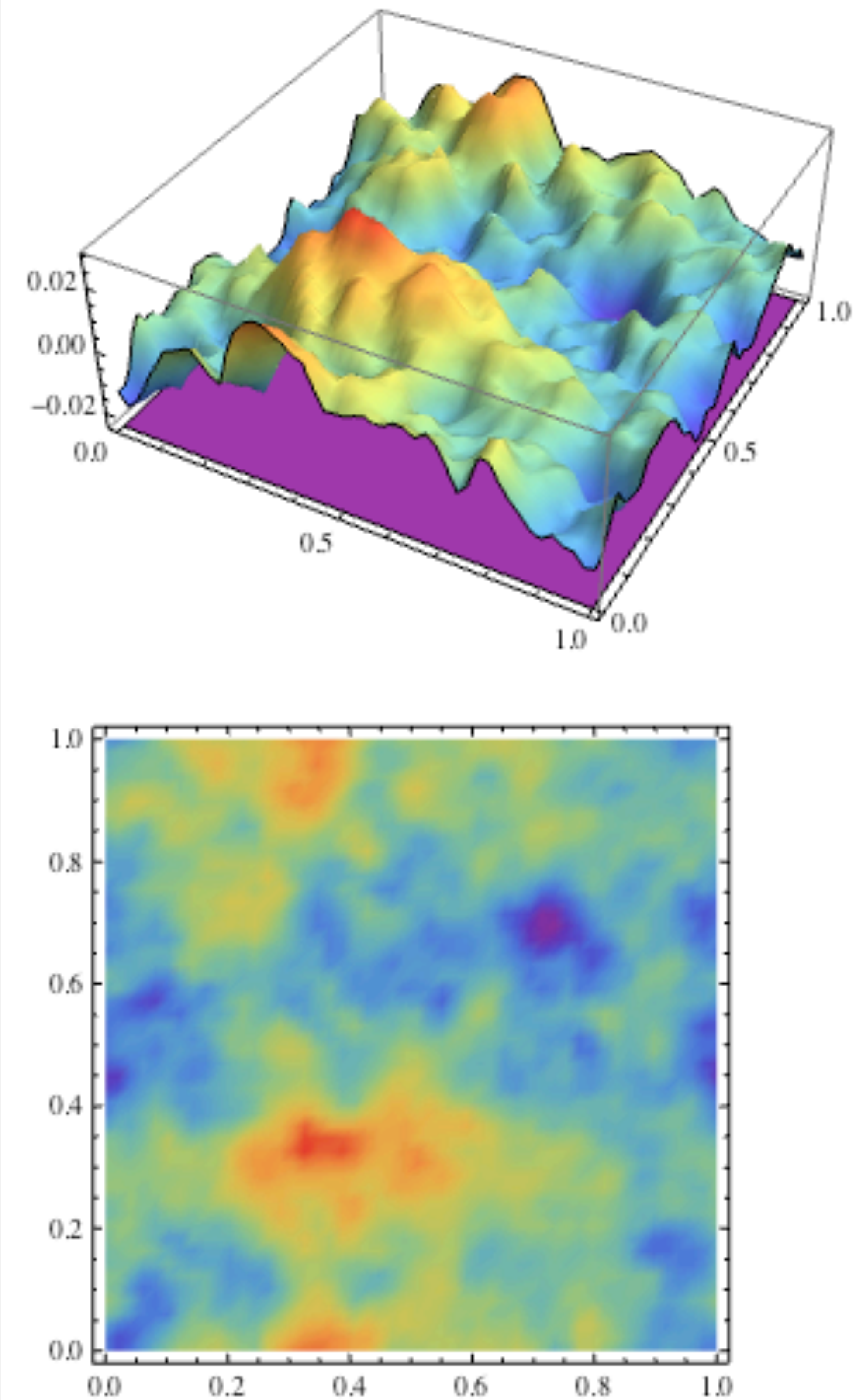

Topological estimators

➢ **Minkowski functionals (topological invariants):**

d+1 MFs in d dimensions.

Mathematical genus in 2D = number of handles/holes (max number of cuttings along closed curves without disconnecting the surface)

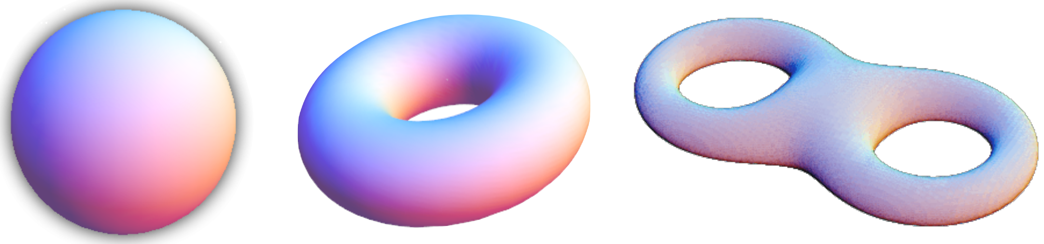

g=0 g=1 g=2

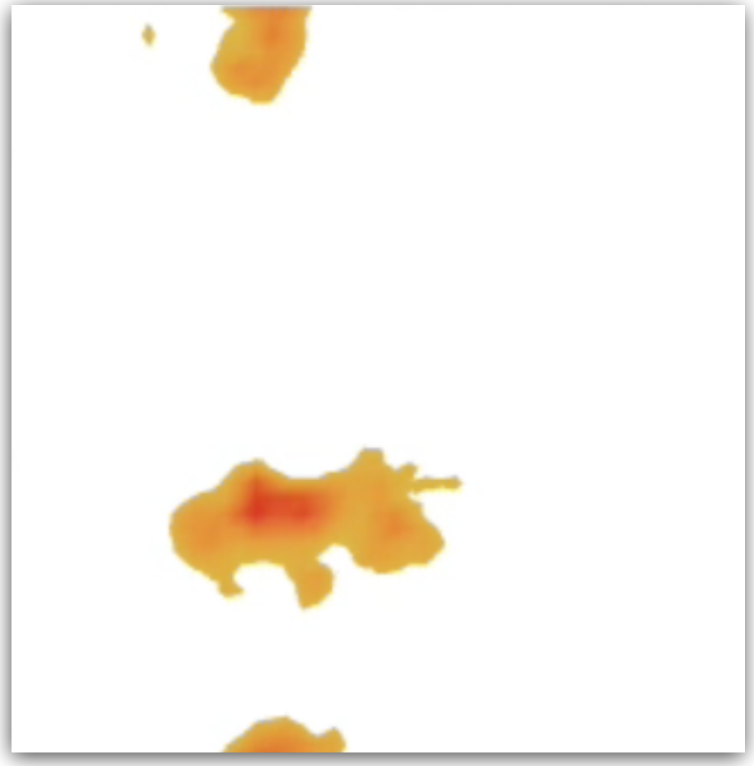

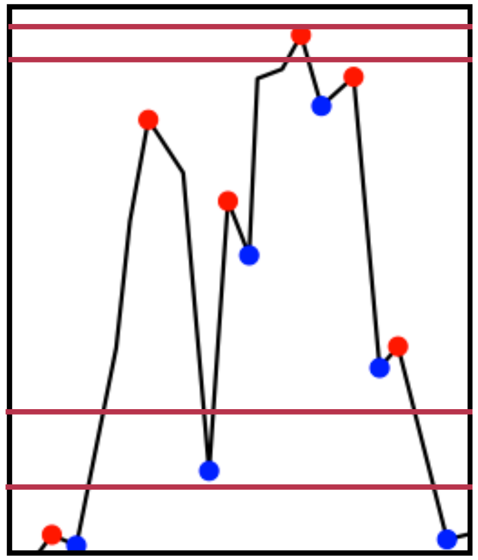

Topological estimators

➢ **Minkowski functionals (topological invariants):**

d+1 MFs in d dimensions.

Mathematical genus in 2D = number of handles/holes (max number of cuttings along closed curves without disconnecting the surface)

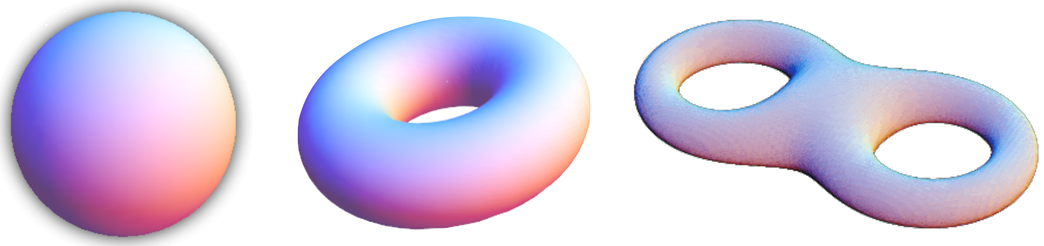

g=0 g=1 g=2

This is a topological invariant: two *surfaces are homeomorphic if they have the same genus.*

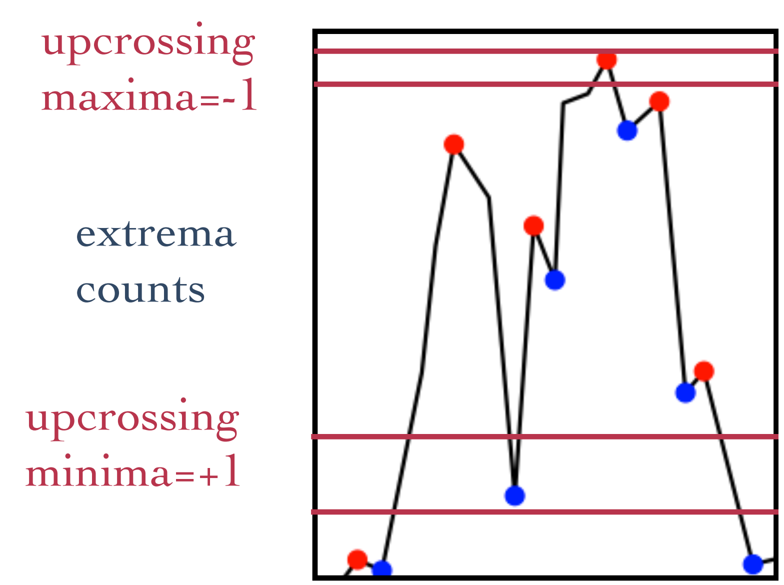

Topological estimators

➢ **Minkowski functionals (topological invariants):**

d+1 MFs in d dimensions.

Mathematical genus in 2D = number of handles/holes (max number of cuttings along closed curves without disconnecting the surface)

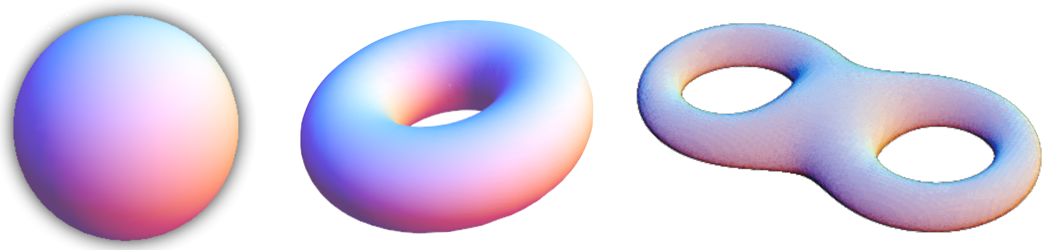

g=0 g=1 g=2

This is a topological invariant: two *surfaces are homeomorphic if they have the same genus.*

In ND, we define the **Euler-Poincaré characteristic** (in 2D, =2-2g) as the alternating sum of Betti numbers:

$$\chi = \sum_i (-1)^i b_i$$

where b_i is its rank of the i-th homology group (b_0=number of connected components, b_1=circular holes, b_2=cavities,…).

Gauss-Bonnet theorem: χ is the integral of the Gaussian curvature

Morse theory: it is the alternating sum of extrema.

The Euler characteristic obeys: **additivity, motion invariance and conditional continuity**, it is one of the MF.

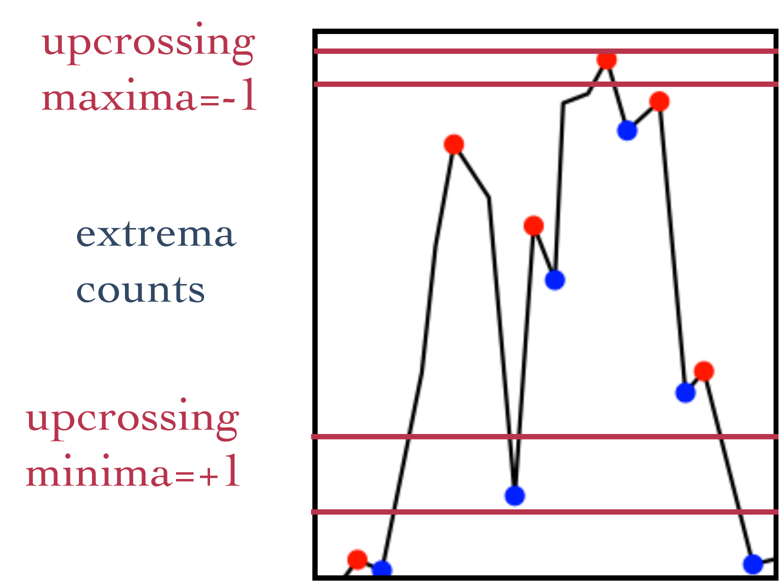

Topological estimators

➢ **Minkowski functionals (topological invariants):**

d+1 MFs in d dimensions: Euler-Poincaré characteristic and??

in 2D: length of isocontour + encompassed volume

in 3D: surface of isocontour+encompassed volume+integrated mean curvature

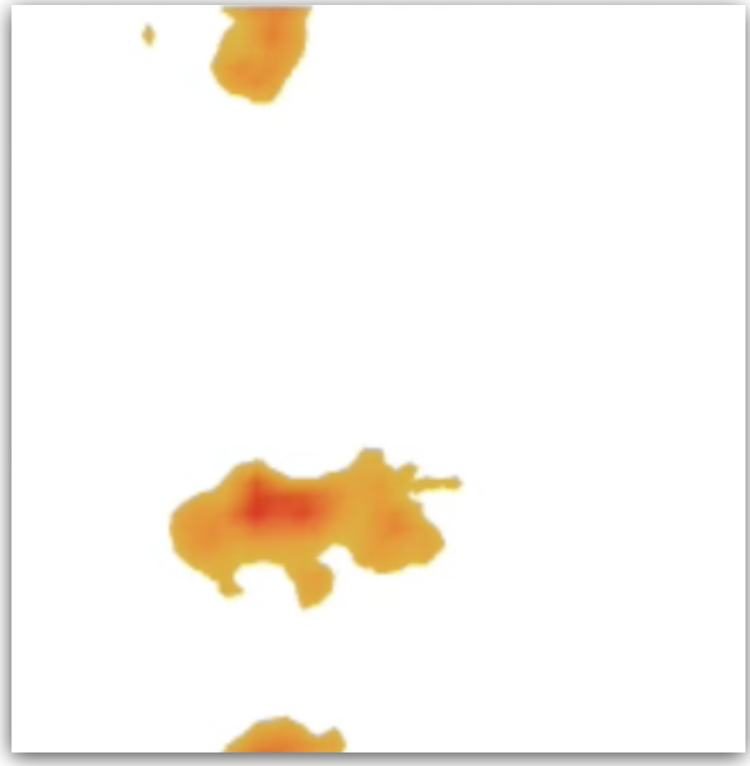

➢ **geometrical estimators and critical sets:**

peak/saddle/void counts

length of filaments

surface of walls

…

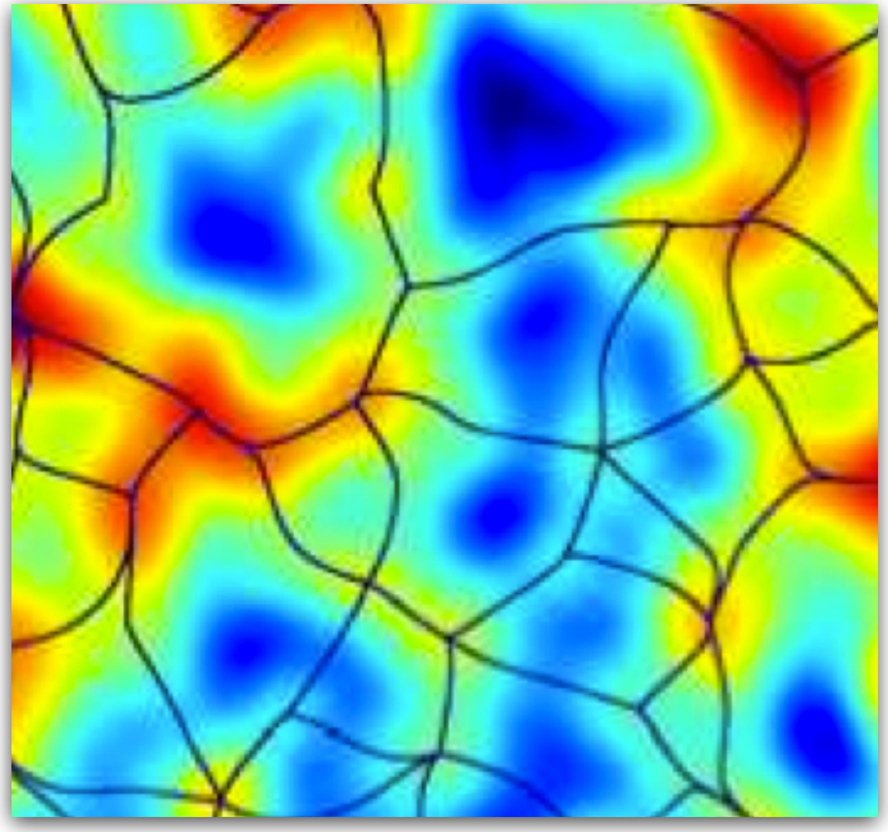

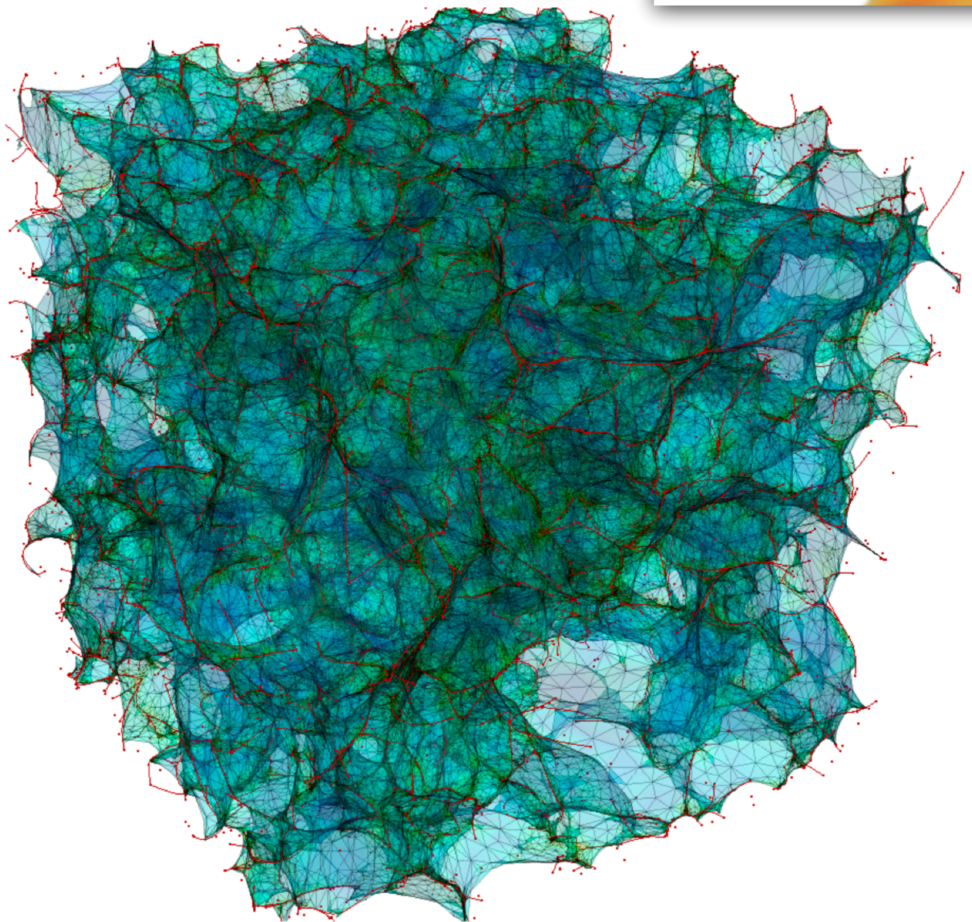

Euler-Poincaré characteristic

$$\chi_{3\mathrm{D}}(\nu) = -\int P(x, x_i, x_{ij}) \delta_{\mathrm{D}}(x_i) \det x_{ij} \Theta(x - \sigma_0 \nu)$$

Using a Gram-Charlier expansion and invariant variables, on can get a prediction to all orders in non-Gaussianity

$$\chi(\nu) = \frac{1}{2}\mathrm{Erfc}\left(\frac{\nu}{\sqrt{2}}\right)\chi(-\infty) + \frac{1}{27R_*^3}\left(\frac{3}{2\pi}\right)^{3/2}\frac{1}{\sqrt{2\pi}}\exp\left(-\frac{\nu^2}{2}\right)\Bigg[\gamma^3 H_2(\nu) +$$
$$+\sum_{n=3}^{\infty}\sum_{i,j,k}^{i+2j+k=n}\frac{(-1)^k}{i!\,j!}\left(-\tfrac{3}{2}\right)^j\left\langle\zeta^i q^{2j} {J_1}^k\right\rangle_{\mathrm{GC}}\left(1-\gamma^2\right)^{i/2}\sum_{s=0}^{\min(3,k)}\frac{3!\gamma^{k+3-2s}}{s!(3-s)!(k-s)!}H_{i+k+2-2s}(\nu)$$
$$+\sum_{n=3}^{\infty}\sum_{i,j,k}^{i+2j+k+2=n}\frac{(-1)^{k+1}3}{i!\,j!}\left(-\tfrac{3}{2}\right)^j\left\langle\zeta^i q^{2j} {J_1}^k J_2\right\rangle_{\mathrm{GC}}\left(1-\gamma^2\right)^{i/2}\sum_{s=0}^{\min(1,k)}\frac{\gamma^{k+1-2s}}{(k-s)!}H_{i+k-2s}(\nu)$$
$$+\sum_{n=3}^{\infty}\sum_{i,j,k}^{i+2j+k+3=n}\frac{(-1)^{k+1}2}{i!\,j!\,k!}\left(-\tfrac{3}{2}\right)^j\left\langle\zeta^i q^{2j} {J_1}^k J_3\right\rangle_{\mathrm{GC}}\left(1-\gamma^2\right)^{i/2}\gamma^k H_{i+k-1}(\nu)\Bigg].$$

Euler-Poincaré characteristic

$$\chi_{3\mathrm{D}}(\nu) = -\int P(x, x_i, x_{ij})\delta_{\mathrm{D}}(x_i)\,\det x_{ij}\Theta(x - \sigma_0\nu)$$

Using a Gram-Charlier expansion and invariant variables, on can get a prediction to all orders in non-Gaussianity

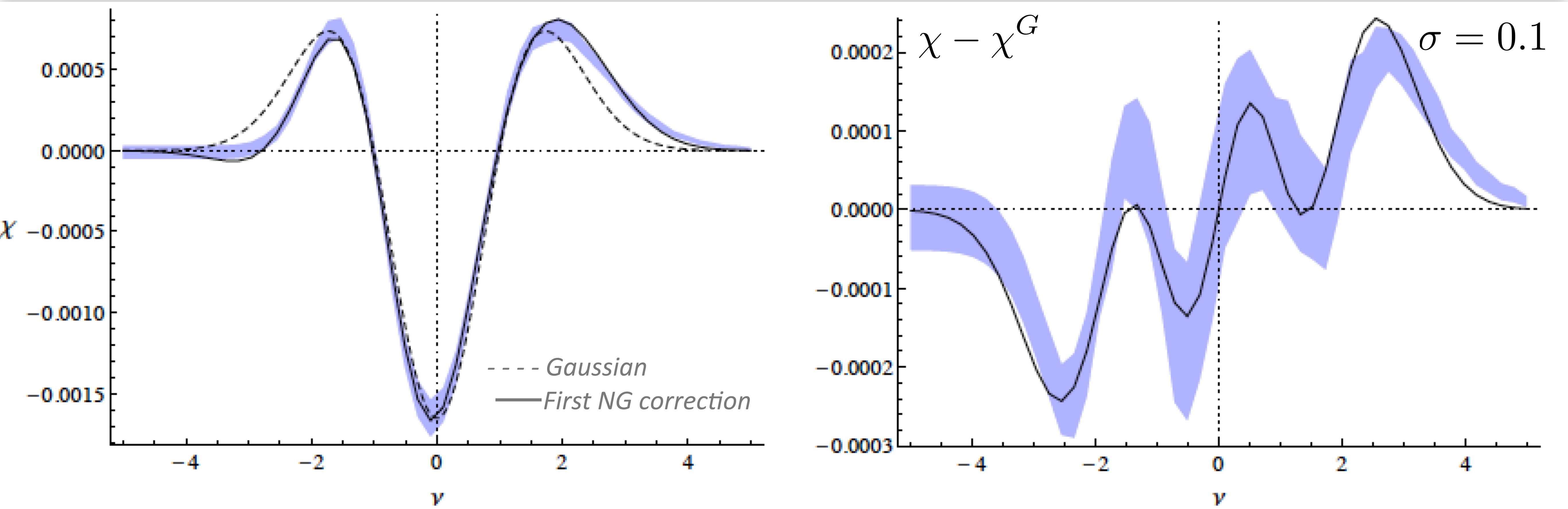

On the connectivity of the cosmic web

- Birth and growth of the cosmic web
- Random fields, Peak theory, topology
- Cosmic connectivity

A 10-year long work with Dmitri Pogosyan (UAlberta) & Christophe Pichon (IAP)

Codis, Pogosyan, Pichon, 2018, MNRAS, 479, 973

Global connectivity for GRF

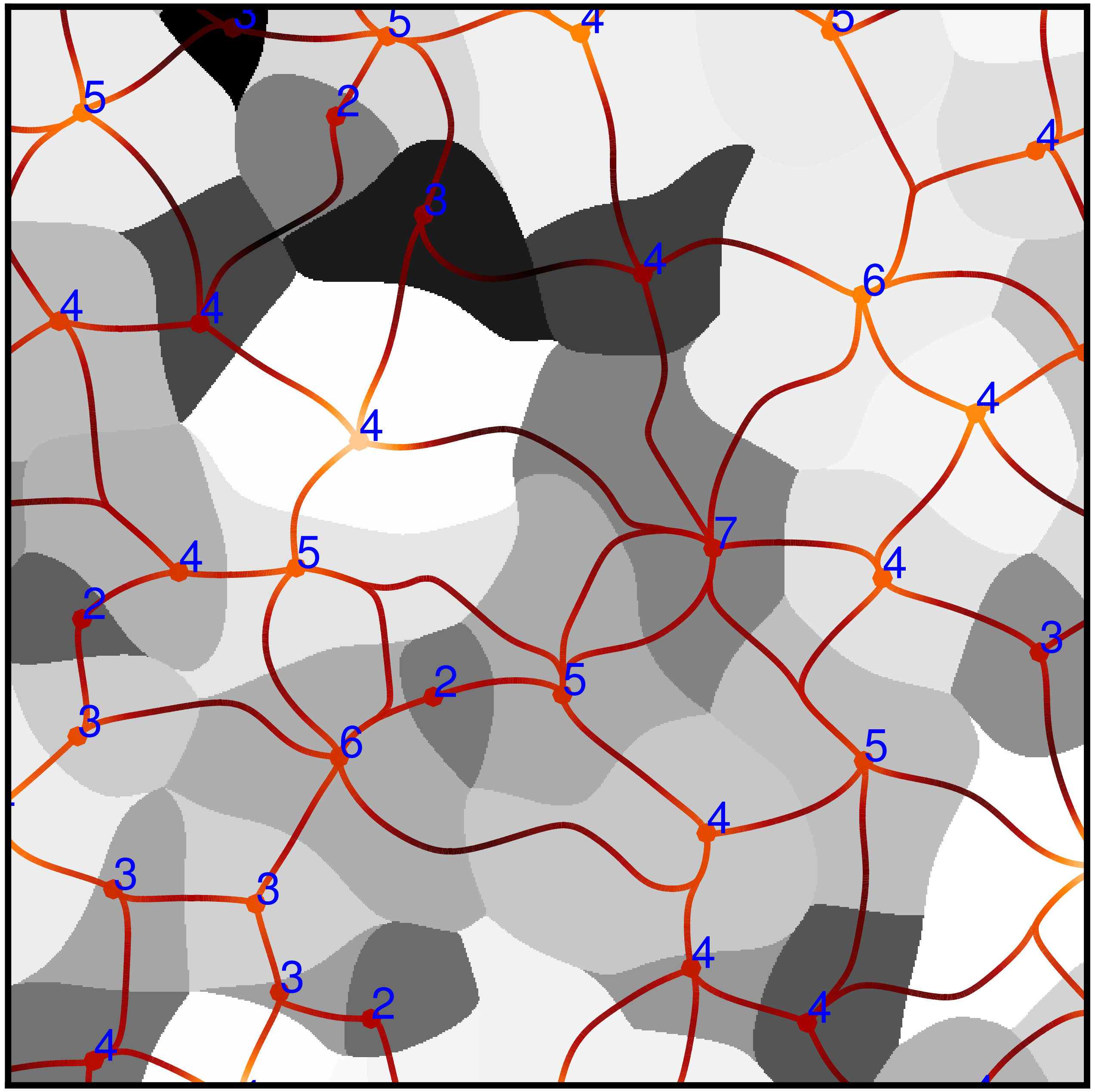

How many filaments connect to a node?

Number of connected saddles are measured using the **Disperse** skeleton algorithm (Soubsie+11) in GRF realisations.

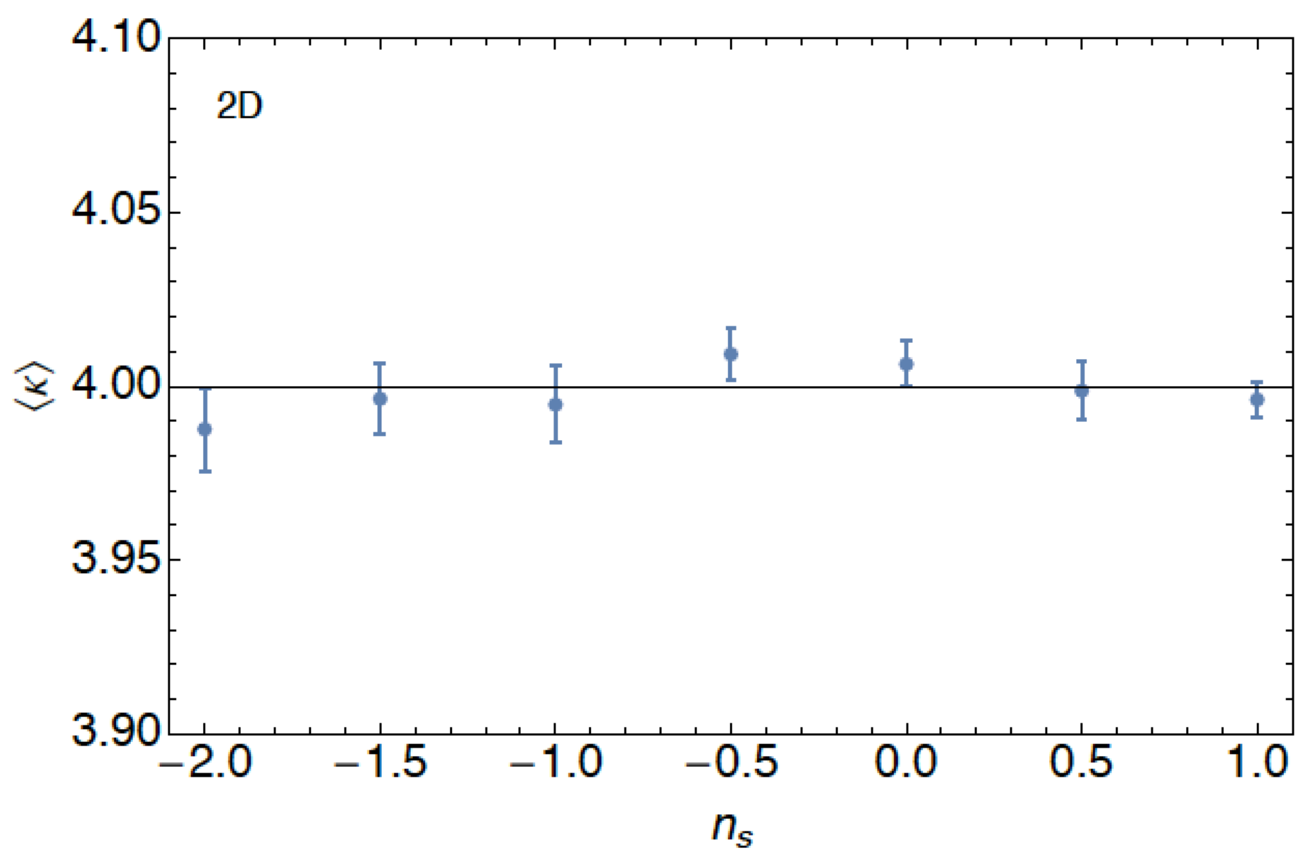

Can we predict the mean connectivity?

Global connectivity for GRF: theory

Because each filament goes through one and only one saddle pt, on average:

$$\langle \kappa \rangle = \frac{2\bar{n}_{\rm sad}}{\bar{n}_{\rm max}}$$

$= 4$ in 2D GRF

$$= \frac{2\left(1057 + 348\sqrt{6}\right)}{625} \approx 6.11 \text{ in 3D GRF}$$

Global connectivity for GRF: theory

Because each filament goes through one and only one saddle pt, on average:

$$\langle \kappa \rangle = \frac{2\bar{n}_{\rm sad}}{\bar{n}_{\rm max}}$$

$= 4$ in 2D GRF

$$= \frac{2\left(1057 + 348\sqrt{6}\right)}{625} \approx 6.11 \quad \text{in 3D GRF}$$

In d dimensions, we relied on numerical integrations:

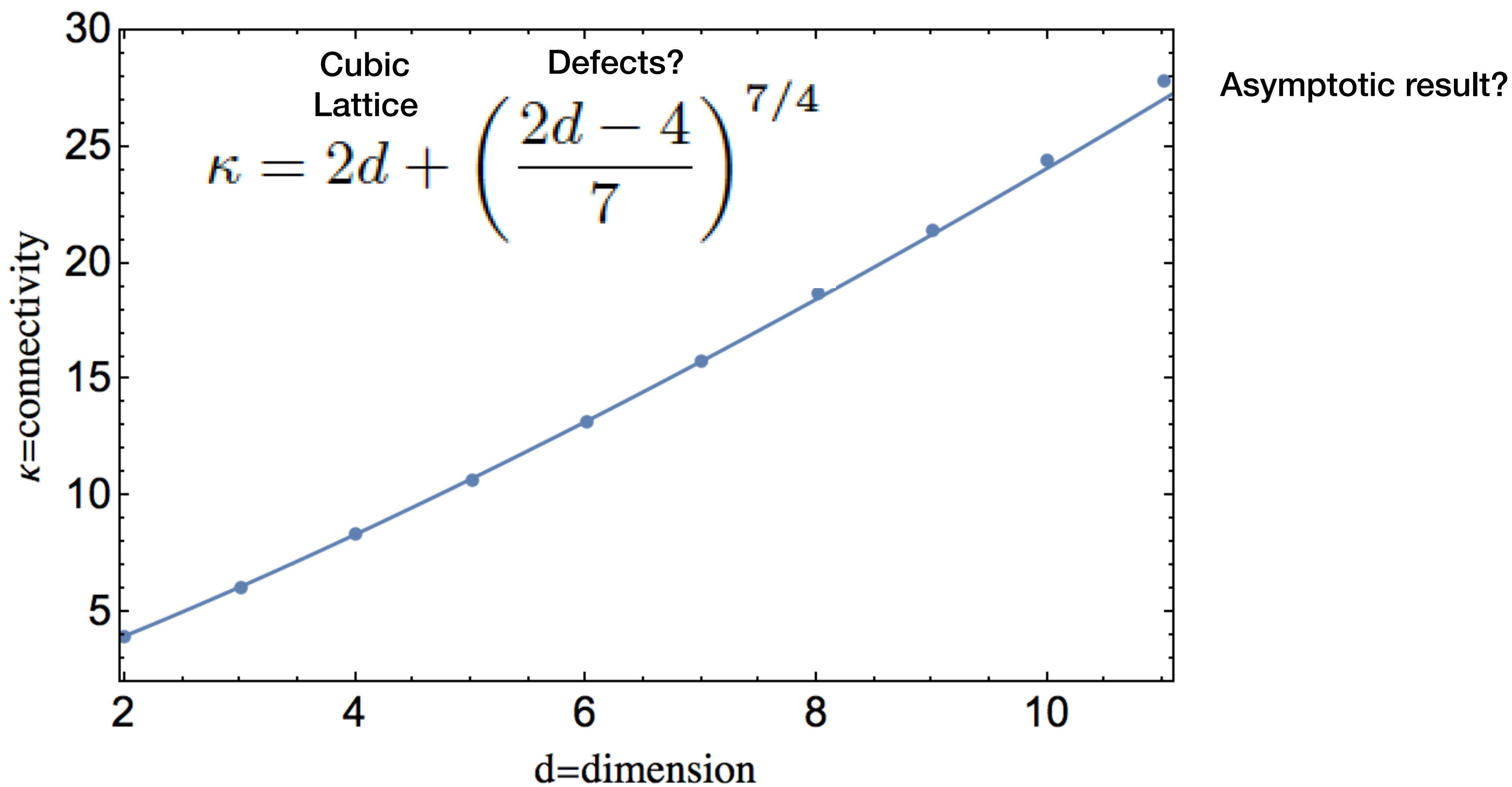

GRF connectivity: dependence with peak height

Full distribution of connectivity:

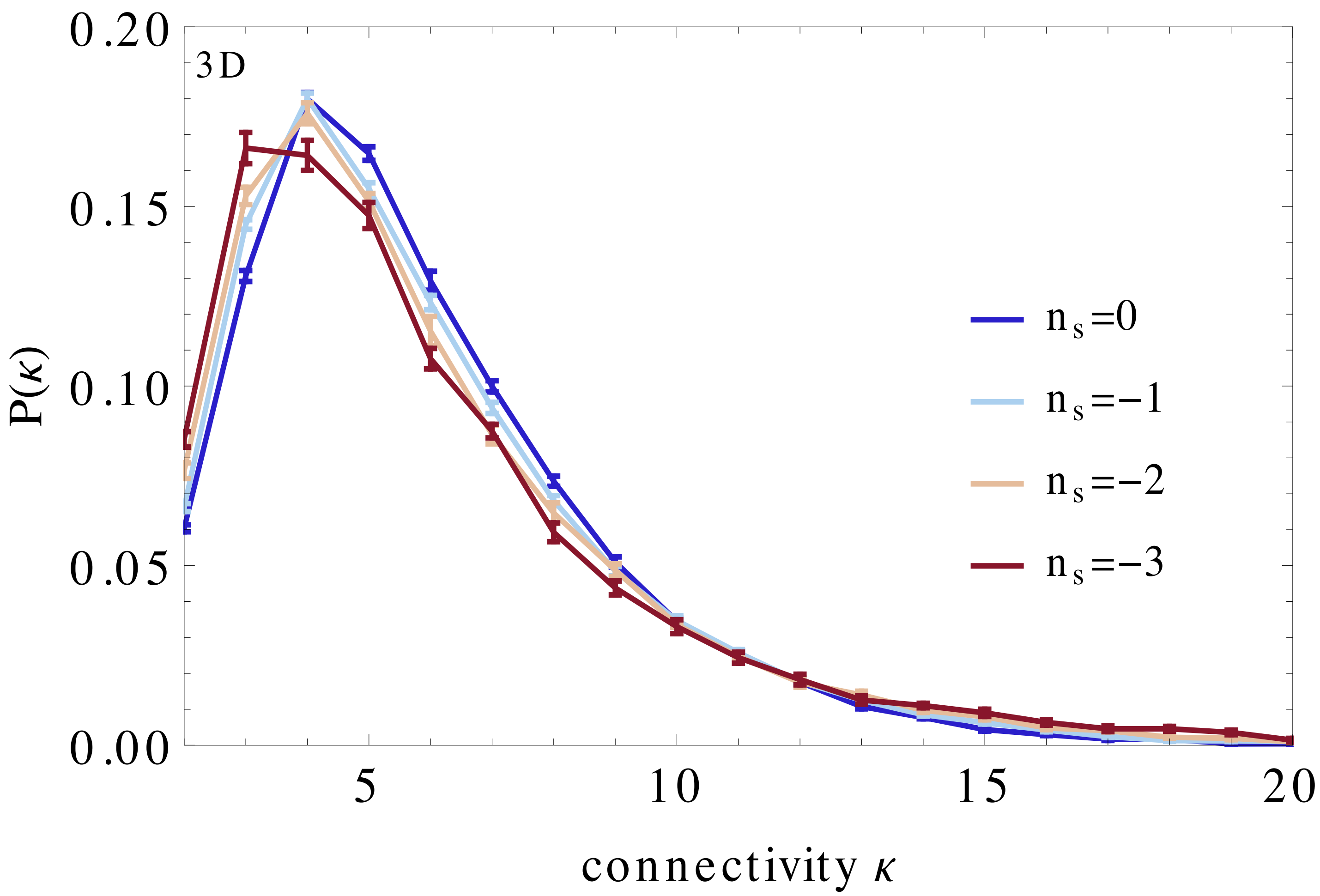

Dependence with peak height:

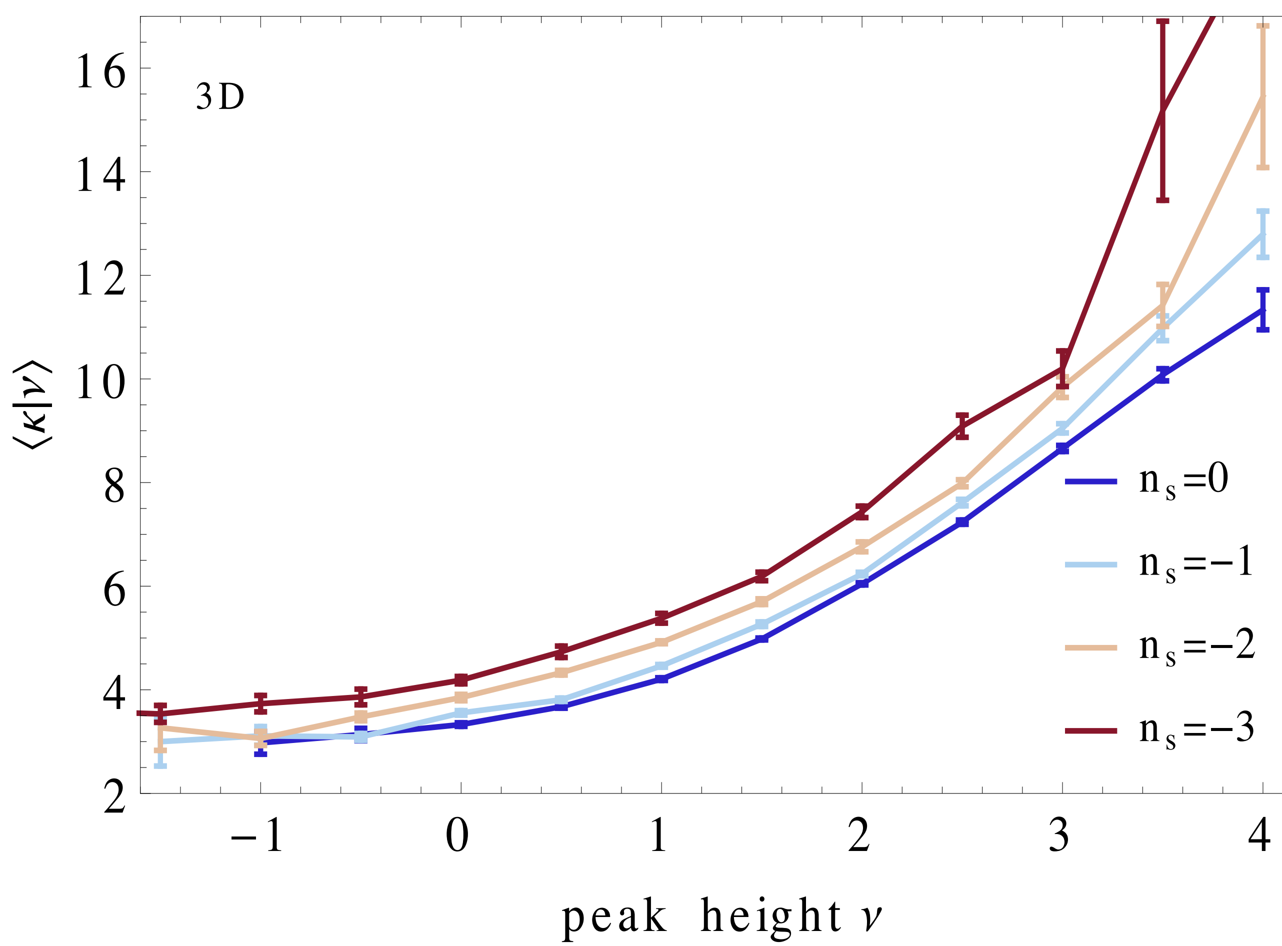

The higher the peak, the more connected

Global connectivity: evolution with cosmic time

- Measurement in cosmological simulations:

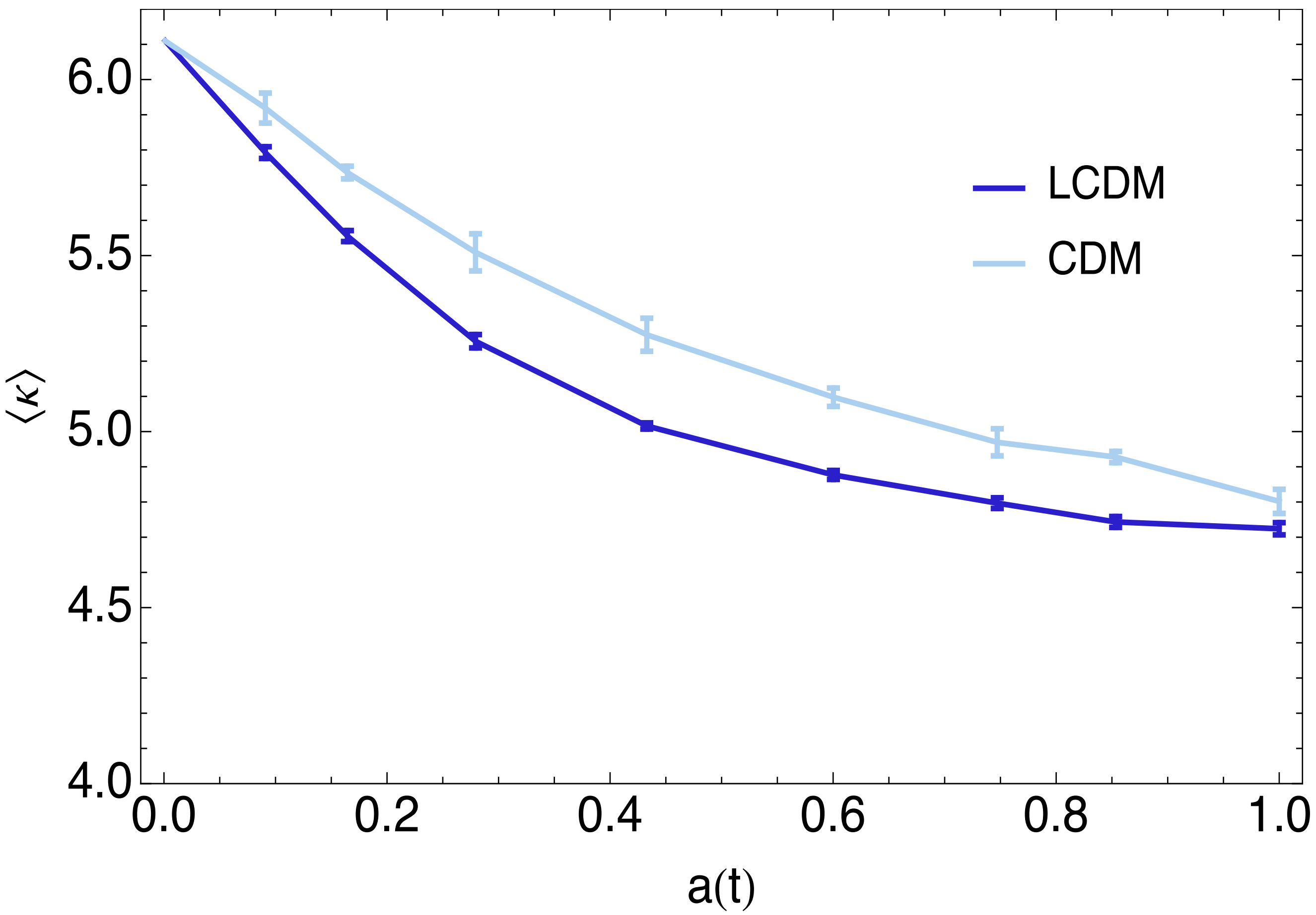

Filaments merge in a cosmology-dependent way!

Global connectivity: evolution with cosmic time

- Measurement in cosmological simulations:

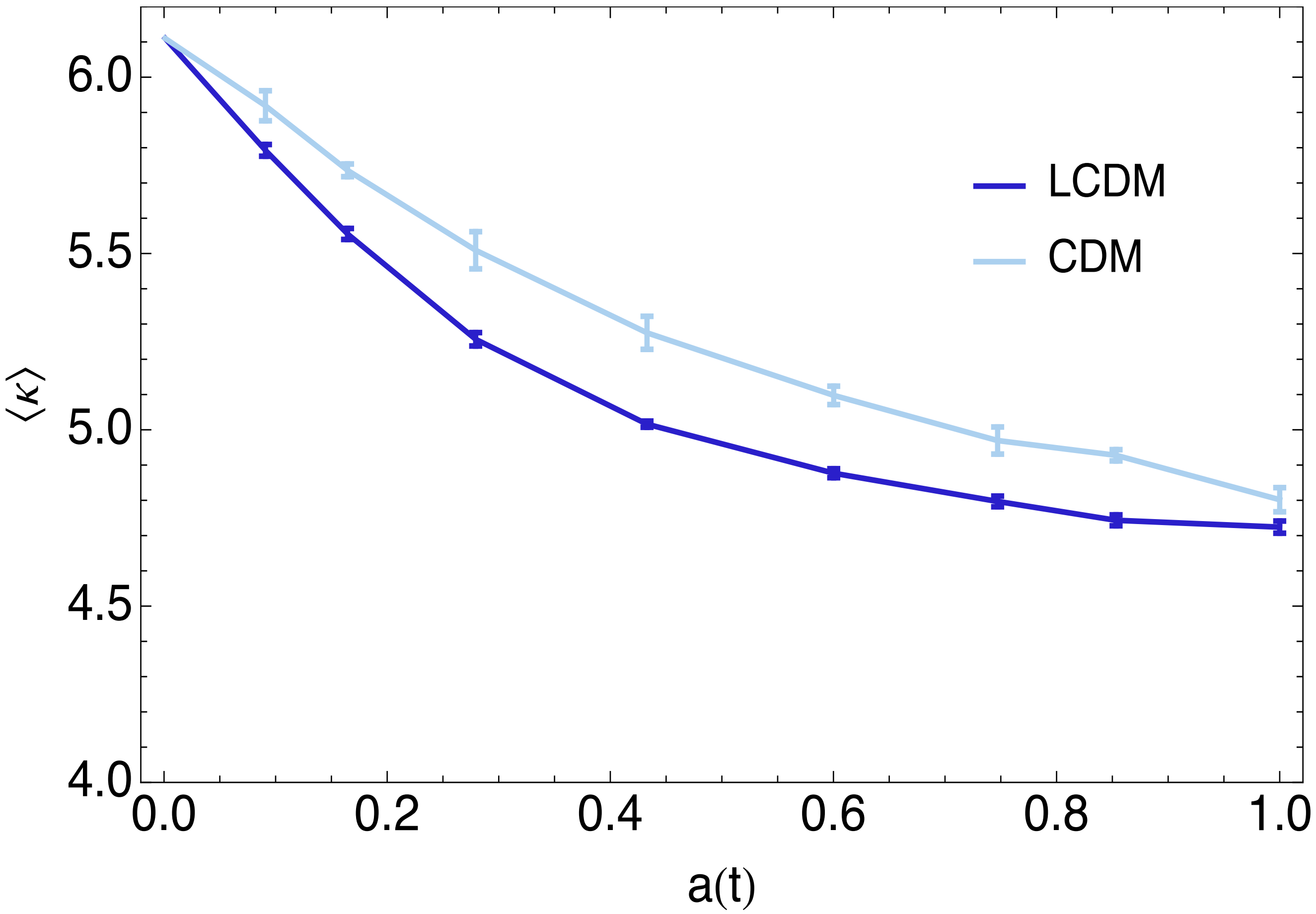

Filaments merge in a cosmology-dependent way!

- Predictions:

Using a Gram Charlier expansion, one can get prediction at arbitrary order in NG

$$\langle\kappa\rangle = \kappa^{\mathrm{G}}\left(1+\sum_{i\geqslant 1}\kappa^{(i)}\sigma_0^i\right)$$

With

$$\kappa^{\mathrm{G}} = 2\times\frac{29\sqrt{3}+18\sqrt{2}}{29\sqrt{3}-18\sqrt{2}}\approx 6.11$$

$$\kappa^{(1)} = \frac{4\sqrt{3}}{35\sqrt{\pi}\sigma_0}\left(8\left\langle J_1^3\right\rangle - 10\left\langle J_1 J_2\right\rangle - 21\left\langle q^2 J_1\right\rangle\right)$$

Local multiplicity and bifurcation points

For galaxy formation, what matters most is how many filament connect **locally** onto a galaxy. At small enough scale, a peak is always **ellipsoidal** so that only two branches of filament stick out. Then those branches **bifurcate**. Some bifurcations appear so close to the peak that they are physically irrelevant. Hence we will define the **multiplicity** as the local number of filaments.

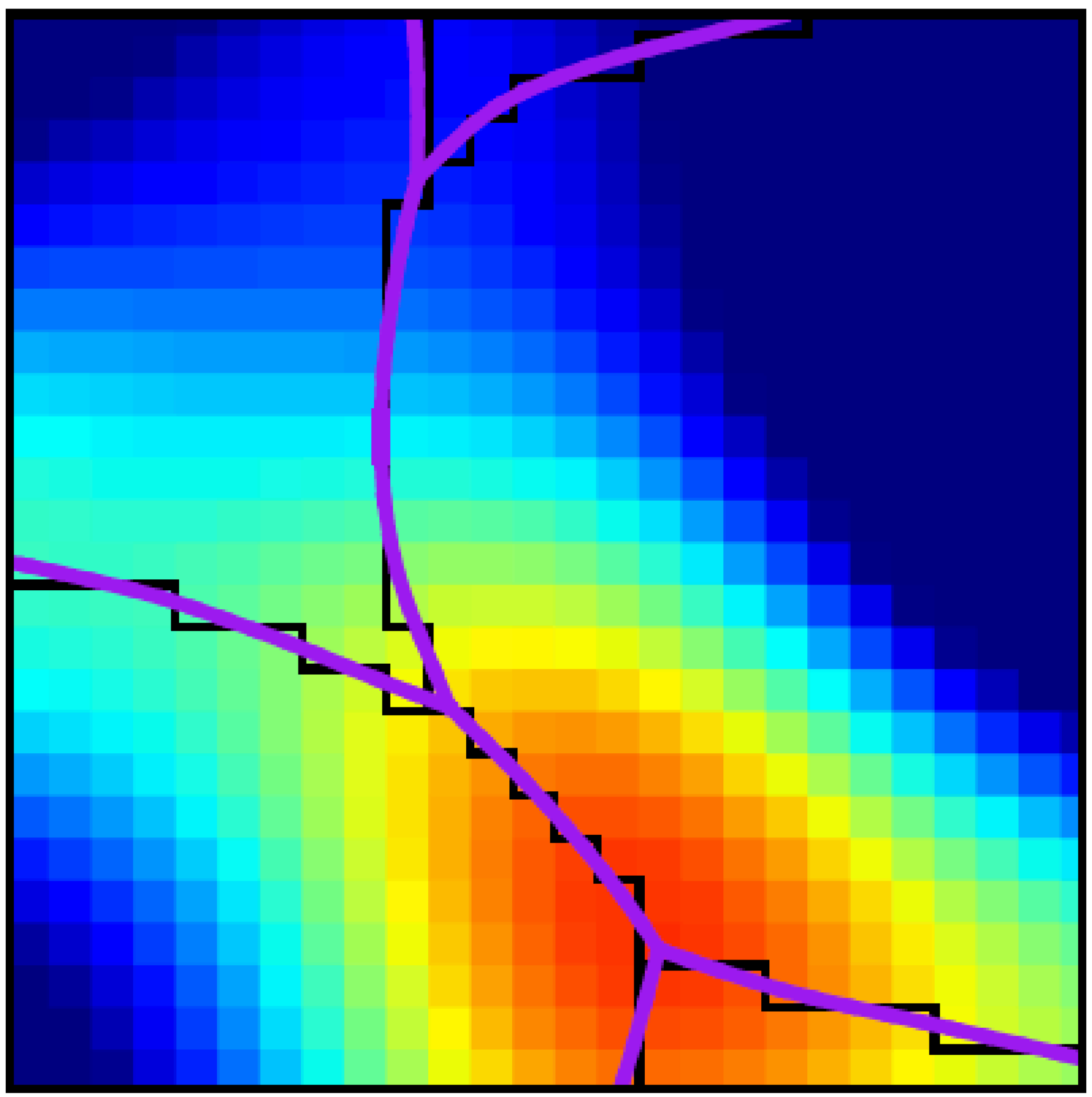

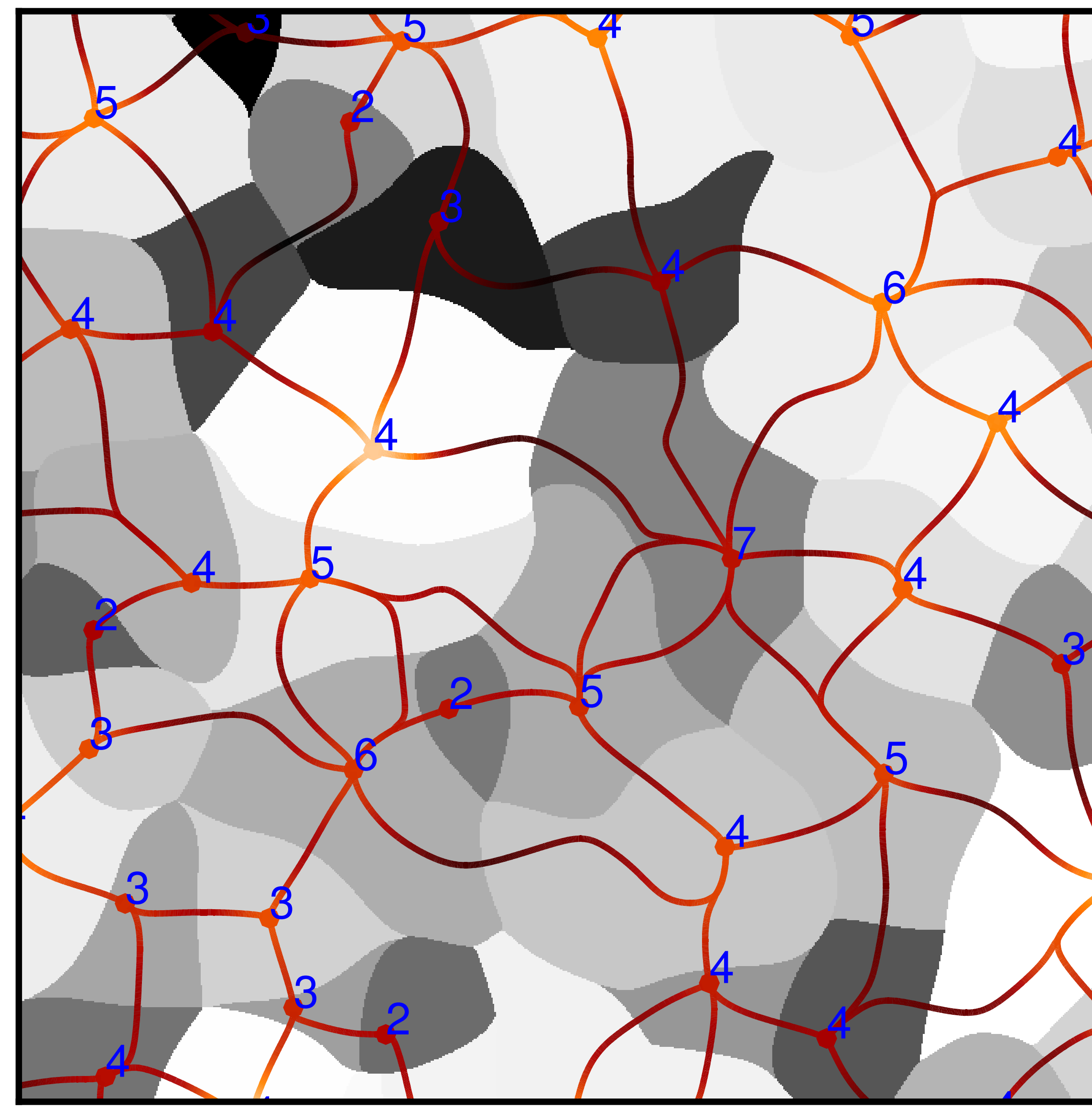

Local multiplicity and bifurcation points

For galaxy formation, what matters most is how many filament connect **locally** onto a galaxy. At small enough scale, a peak is always **ellipsoidal** so that only two branches of filament stick out. Then those branches **bifurcate**. Some bifurcations appear so close to the peak that they are physically irrelevant. Hence we will define the **multiplicity** as the local number of filaments.

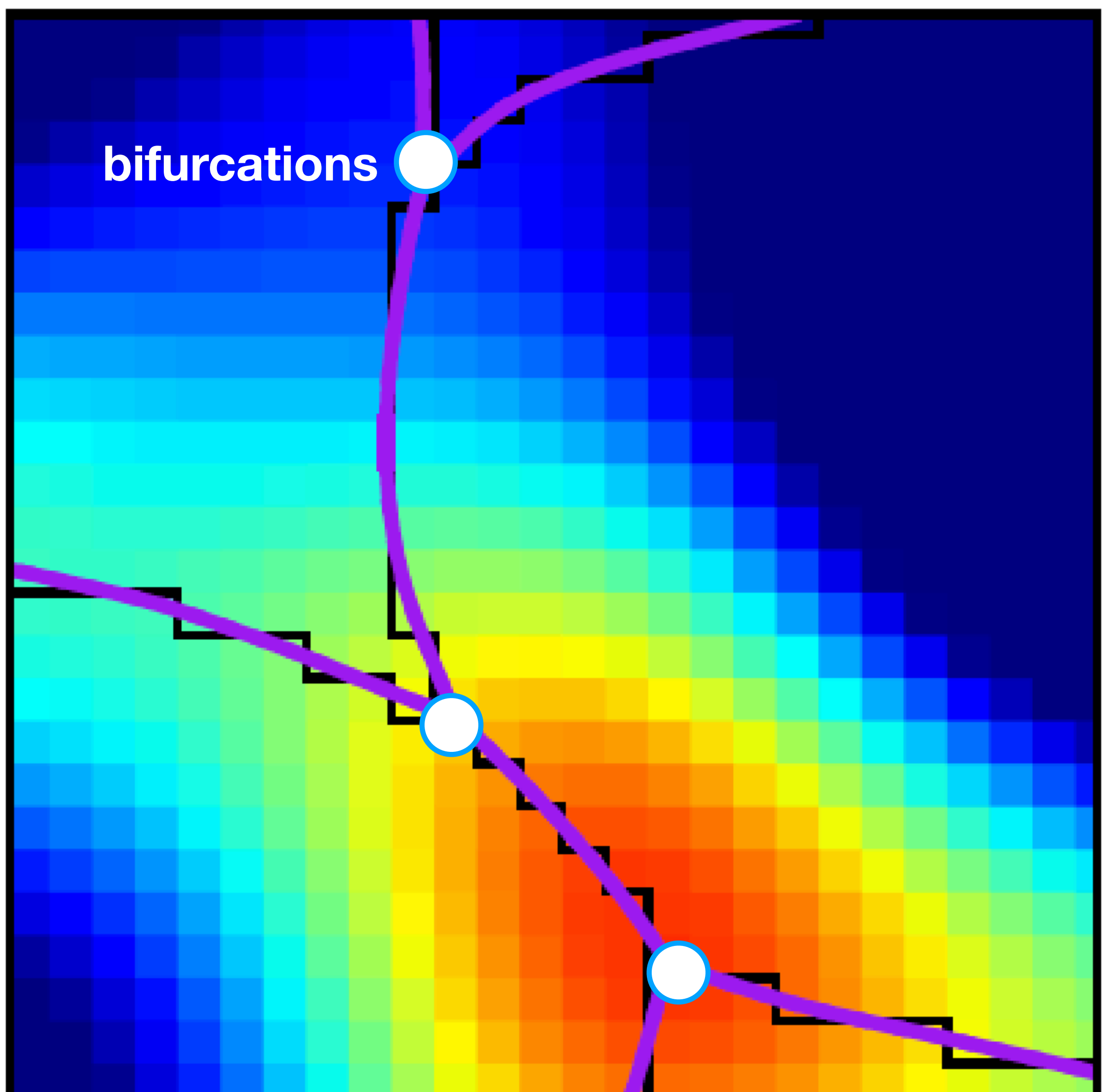

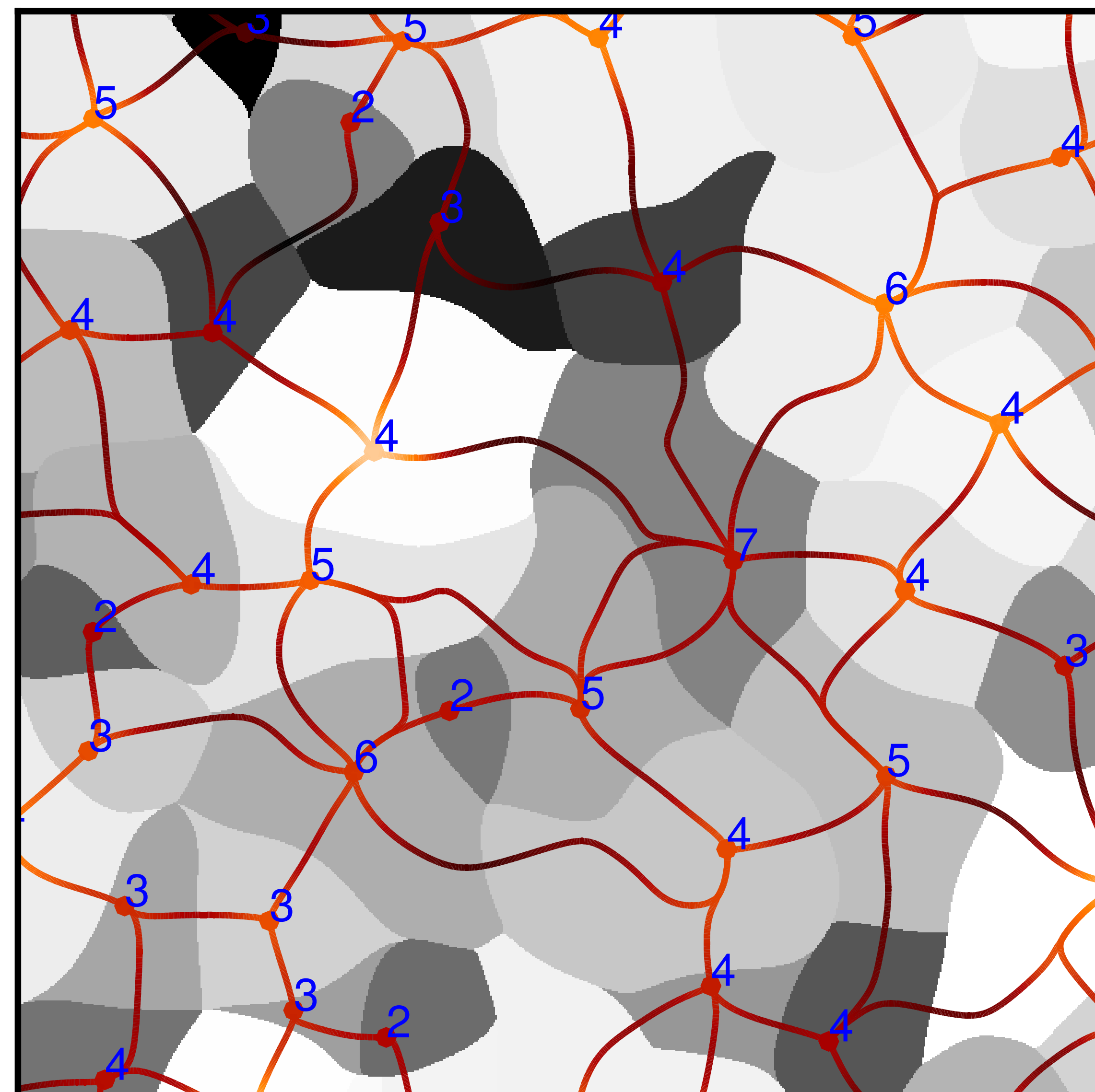

Local multiplicity and bifurcation points

For galaxy formation, what matters most is how many filament connect **locally** onto a galaxy. At small enough scale, a peak is always **ellipsoidal** so that only two branches of filament stick out. Then those branches **bifurcate**. Some bifurcations appear so close to the peak that they are physically irrelevant. Hence we will define the **multiplicity** as the local number of filaments.

$$\mu = \kappa - n_{\mathrm{bifurcations}}$$

$\mu \approx 3$ in 2D

$\mu \approx 4$ in 3D

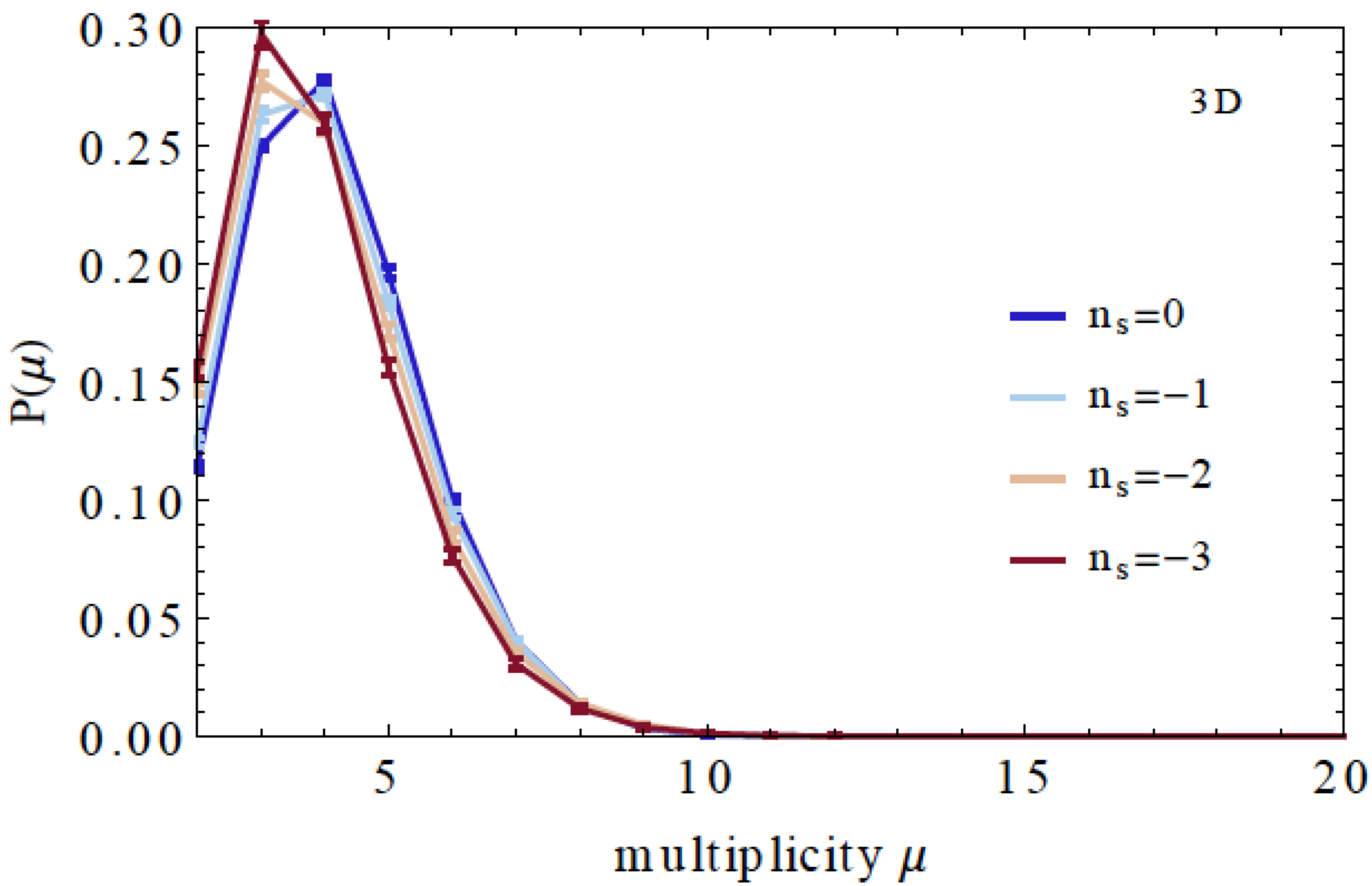

Local multiplicity

The denser the environment, the higher the multiplicity therefore bringing less coherent angular momentum and generating more ellipsoidal galaxies?

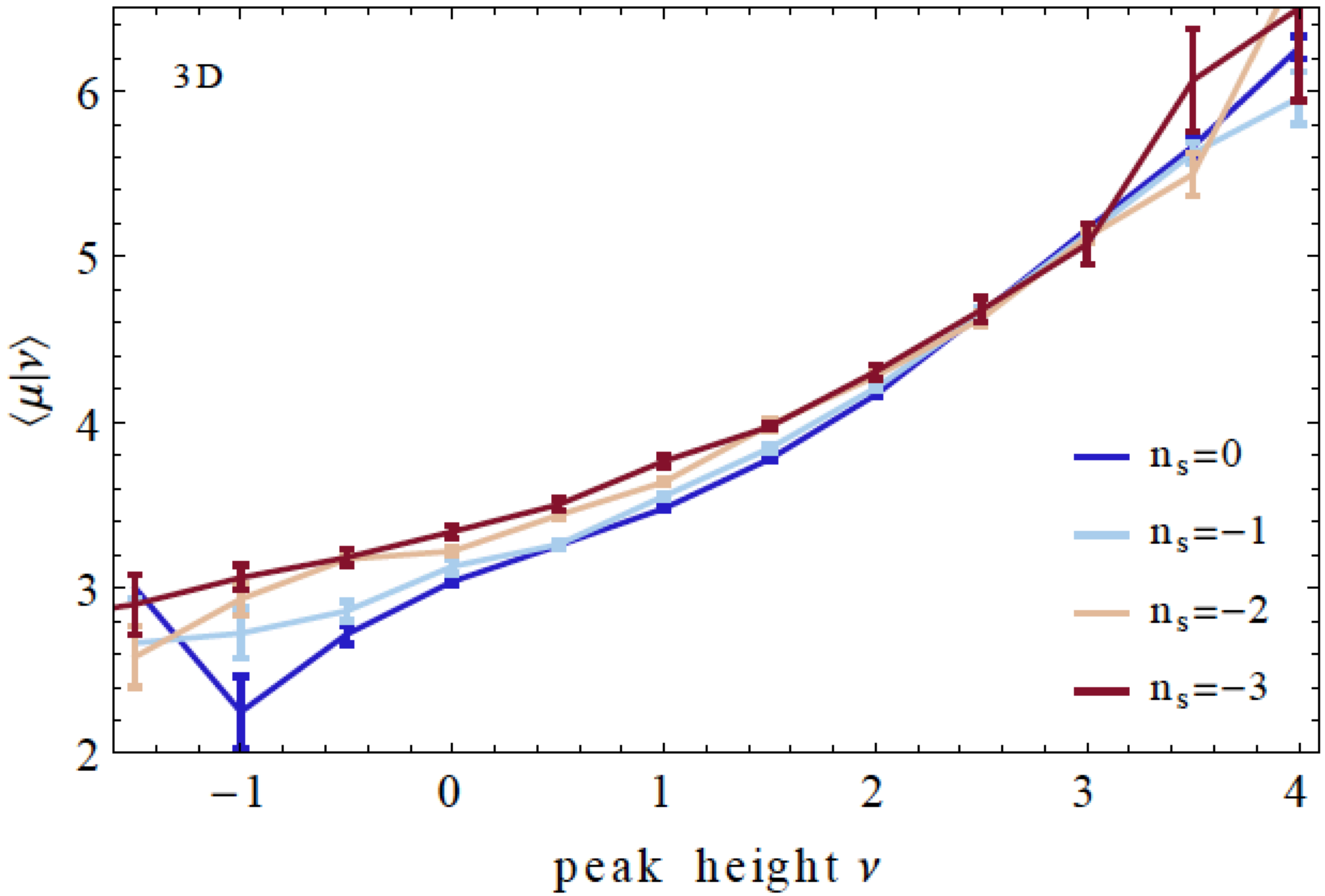

Local multiplicity

The denser the environment, the higher the multiplicity therefore bringing less coherent angular momentum and generating more ellipsoidal galaxies?

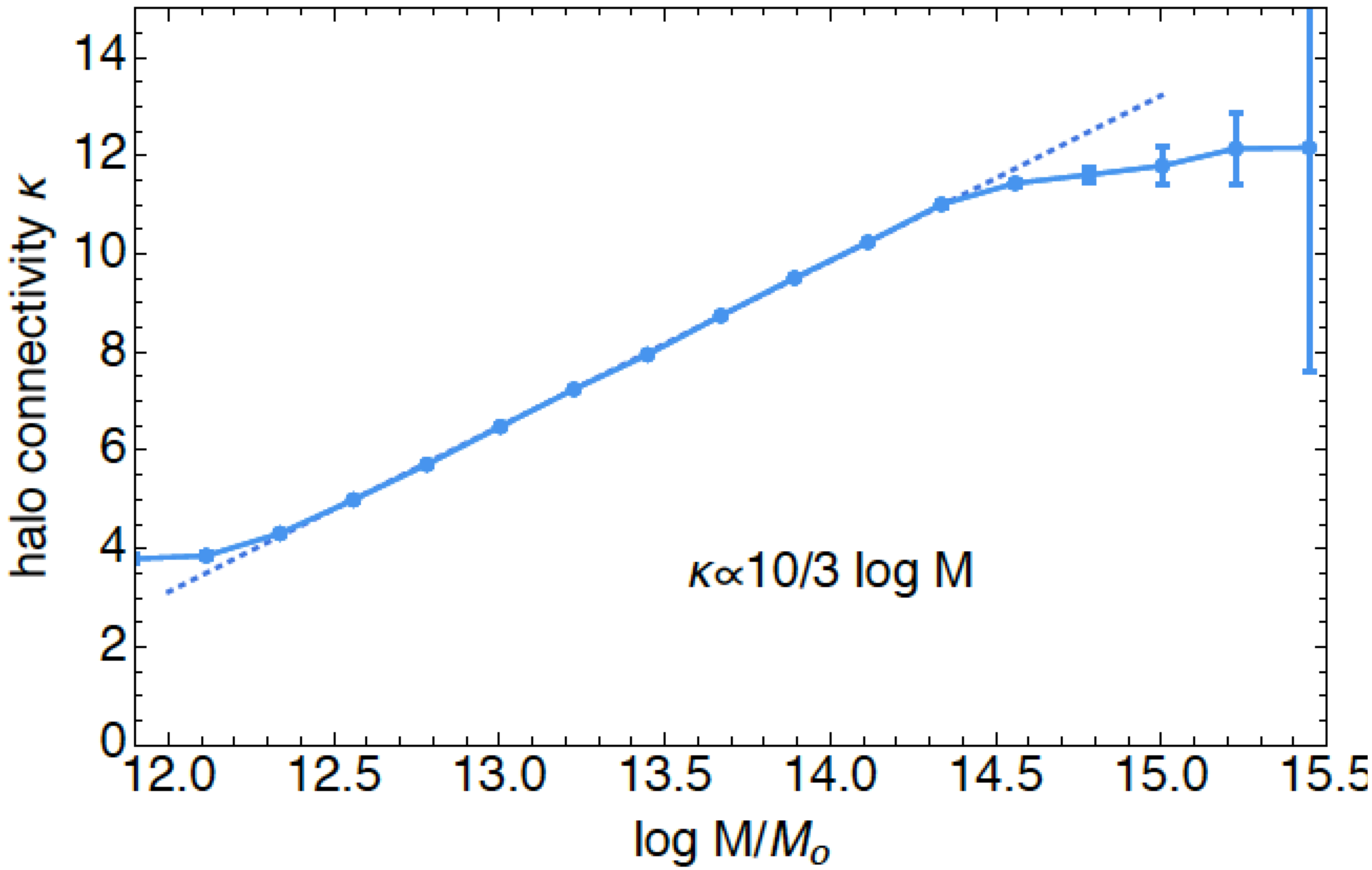

Work in progress…

Local multiplicity: towards a theoretical prediction

Let us count filament crossings at a sphere of radius R around the central peak…

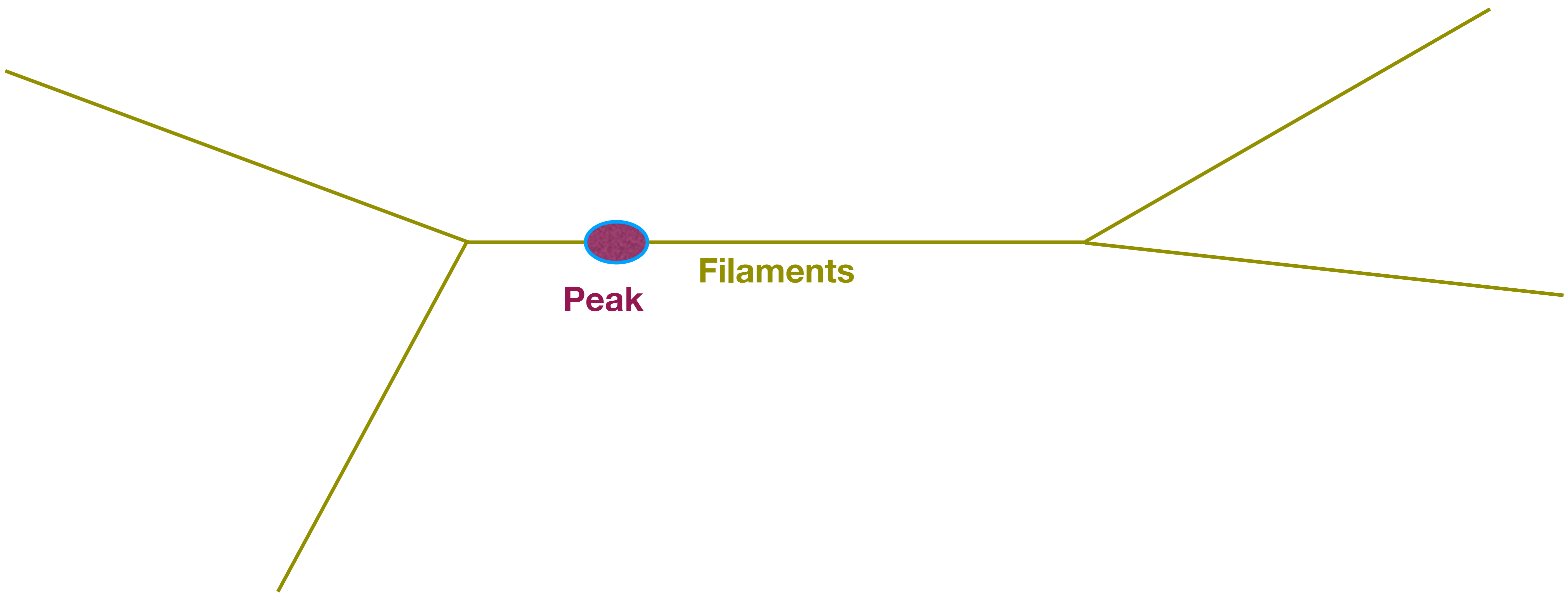

Local multiplicity: towards a theoretical prediction

Let us count filament crossings at a sphere of radius R around the central peak…

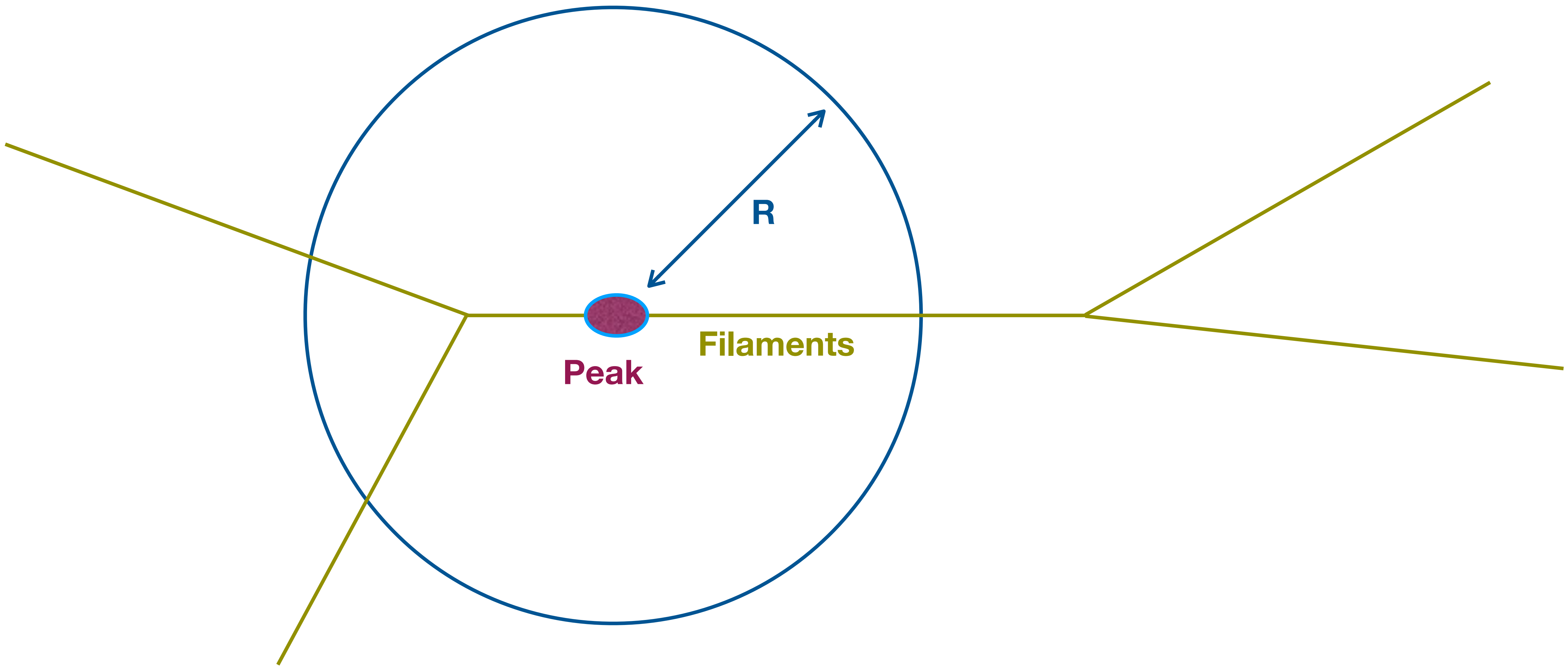

Local multiplicity: towards a theoretical prediction

Let us count filament crossings at a sphere of radius R around the central peak…

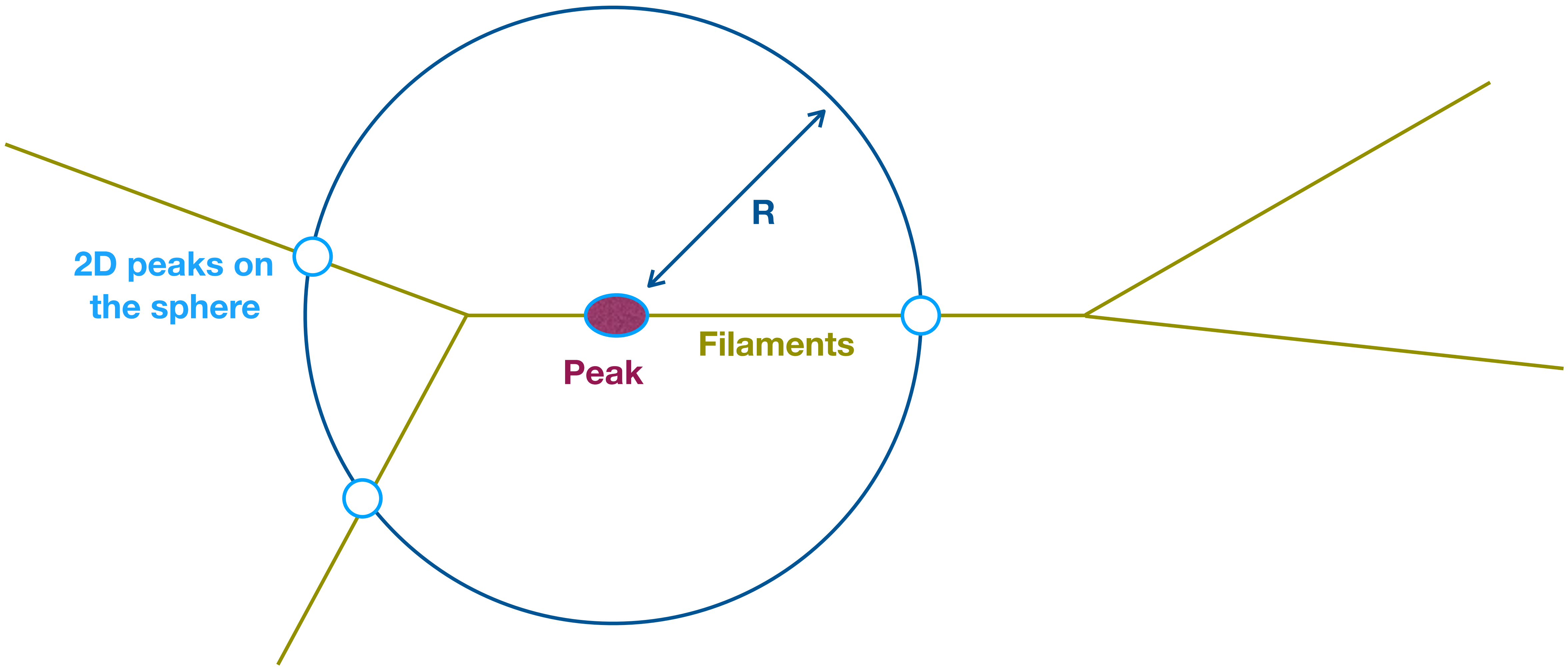

Local multiplicity: towards a theoretical prediction

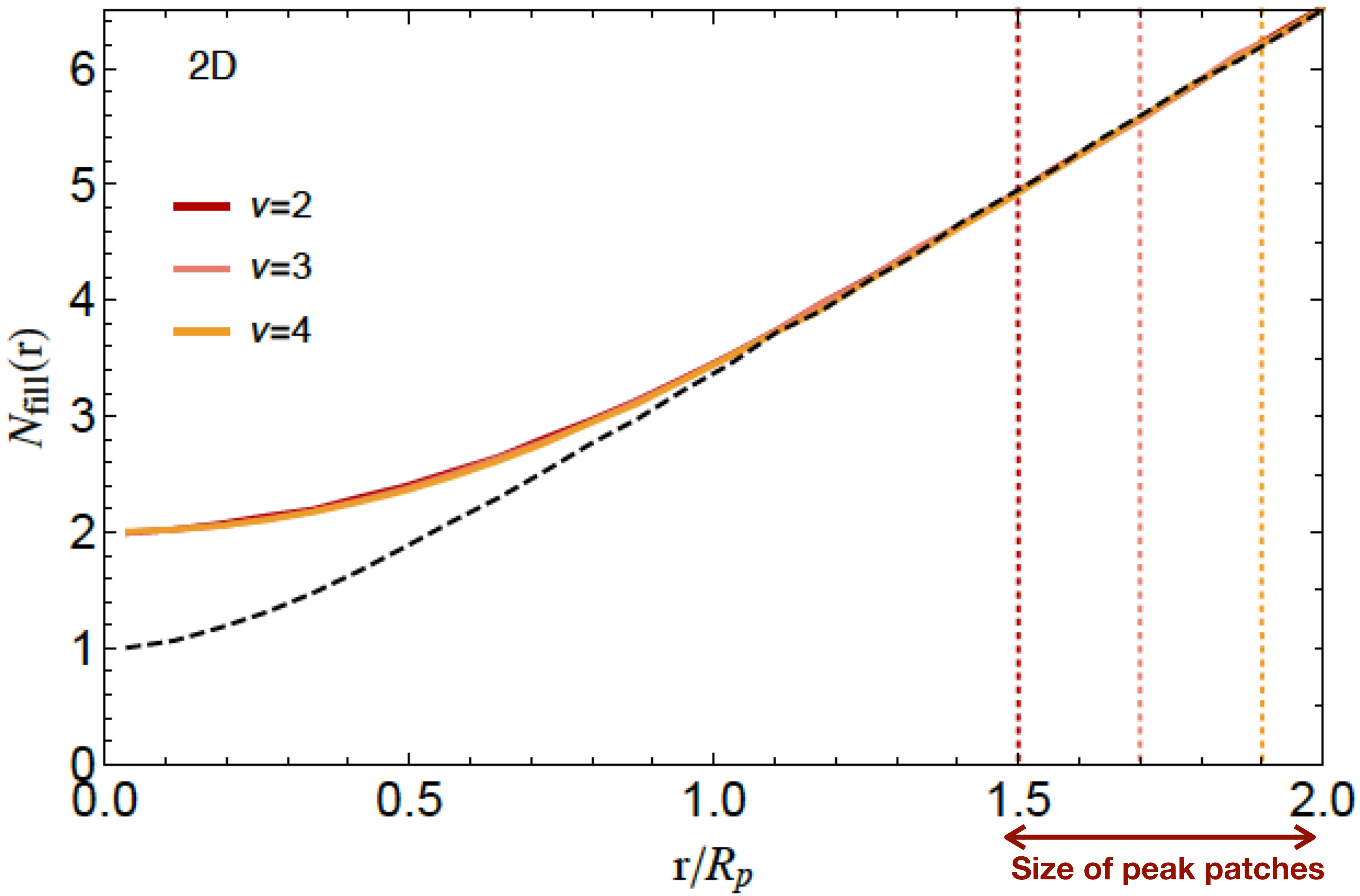

Size of peak patches
depends on their height

Local multiplicity: towards a theoretical prediction

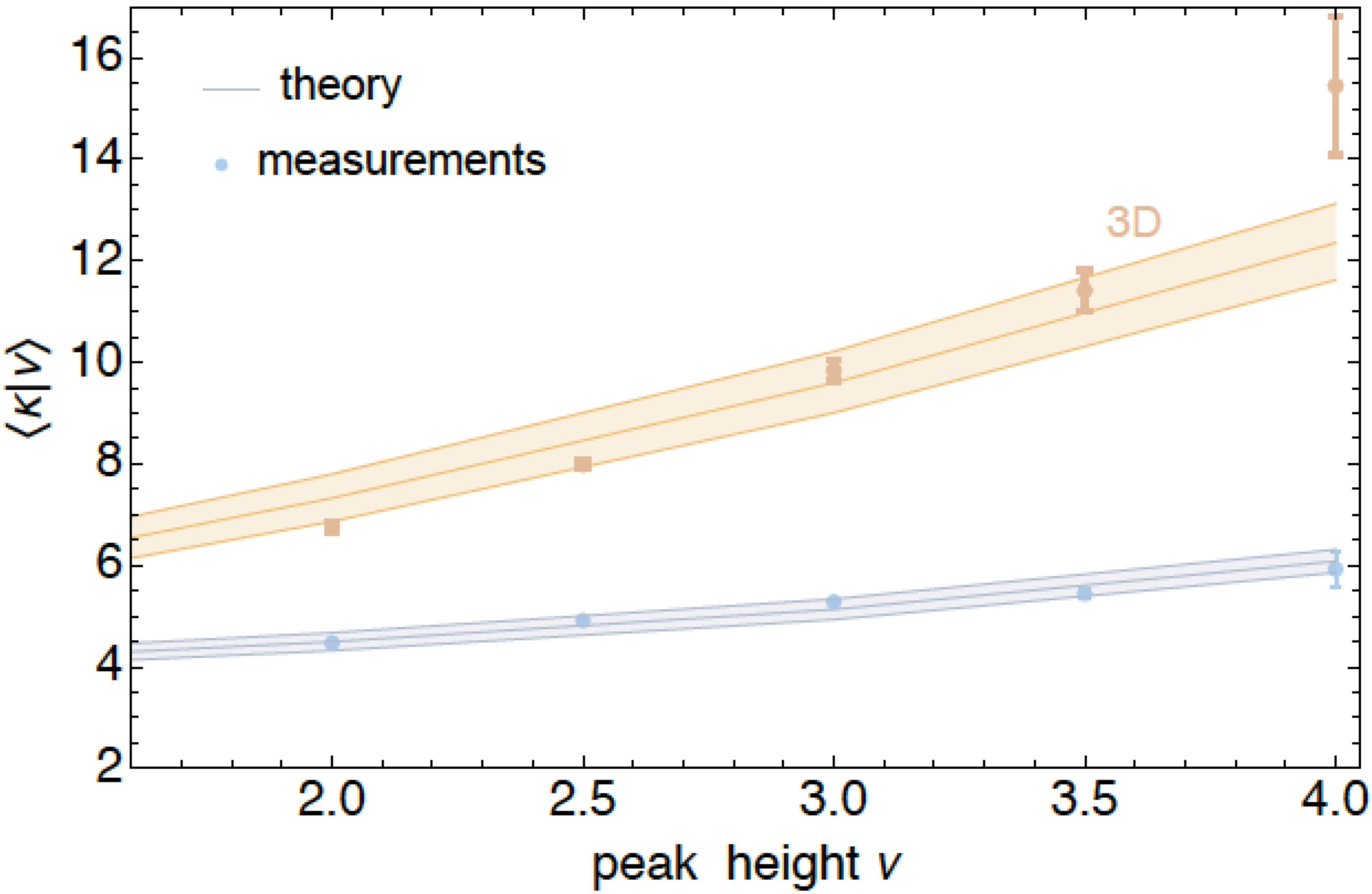

Local multiplicity: towards a theoretical prediction

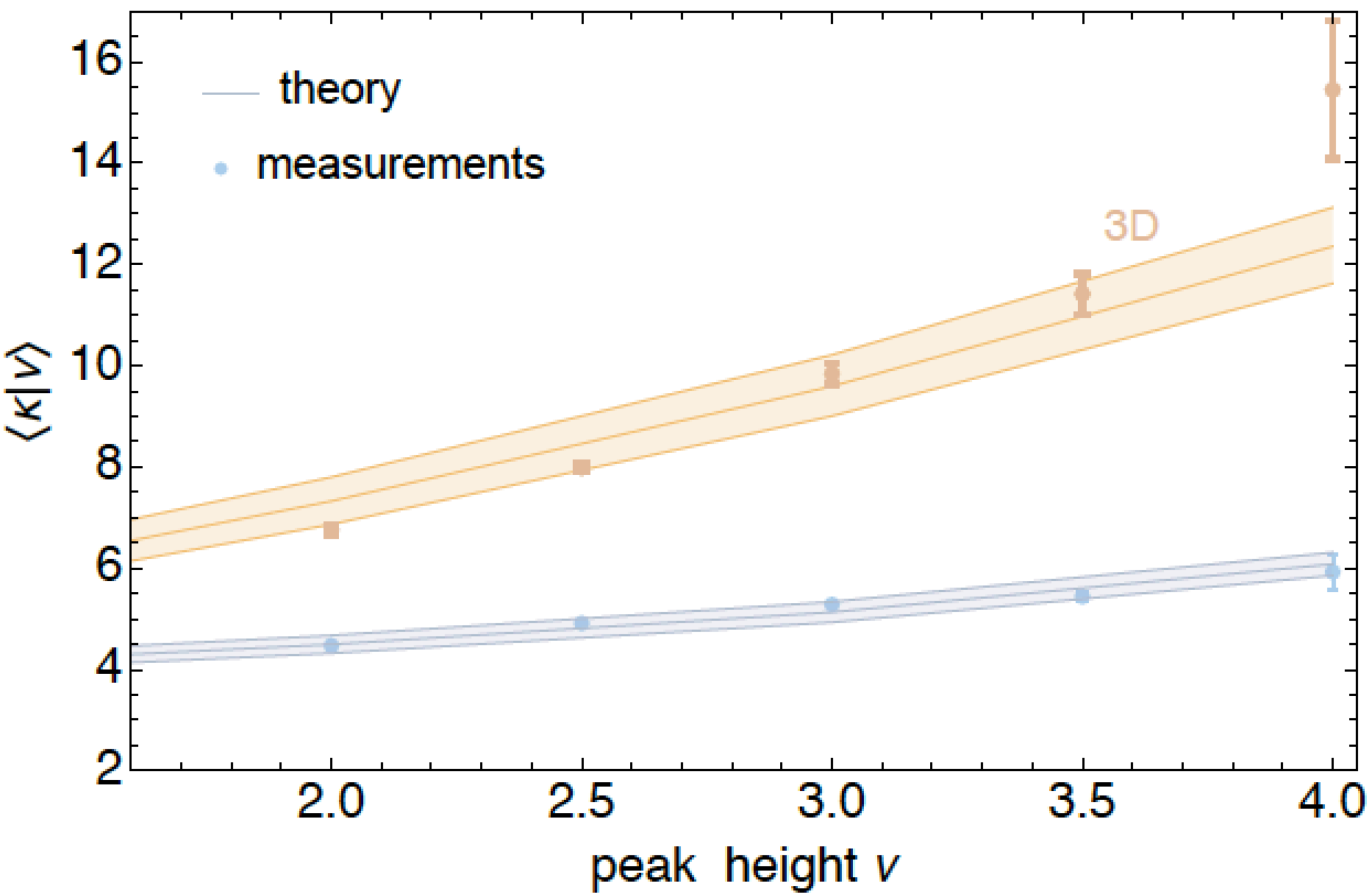

But how dense are those filaments?

Local multiplicity: towards a theoretical prediction

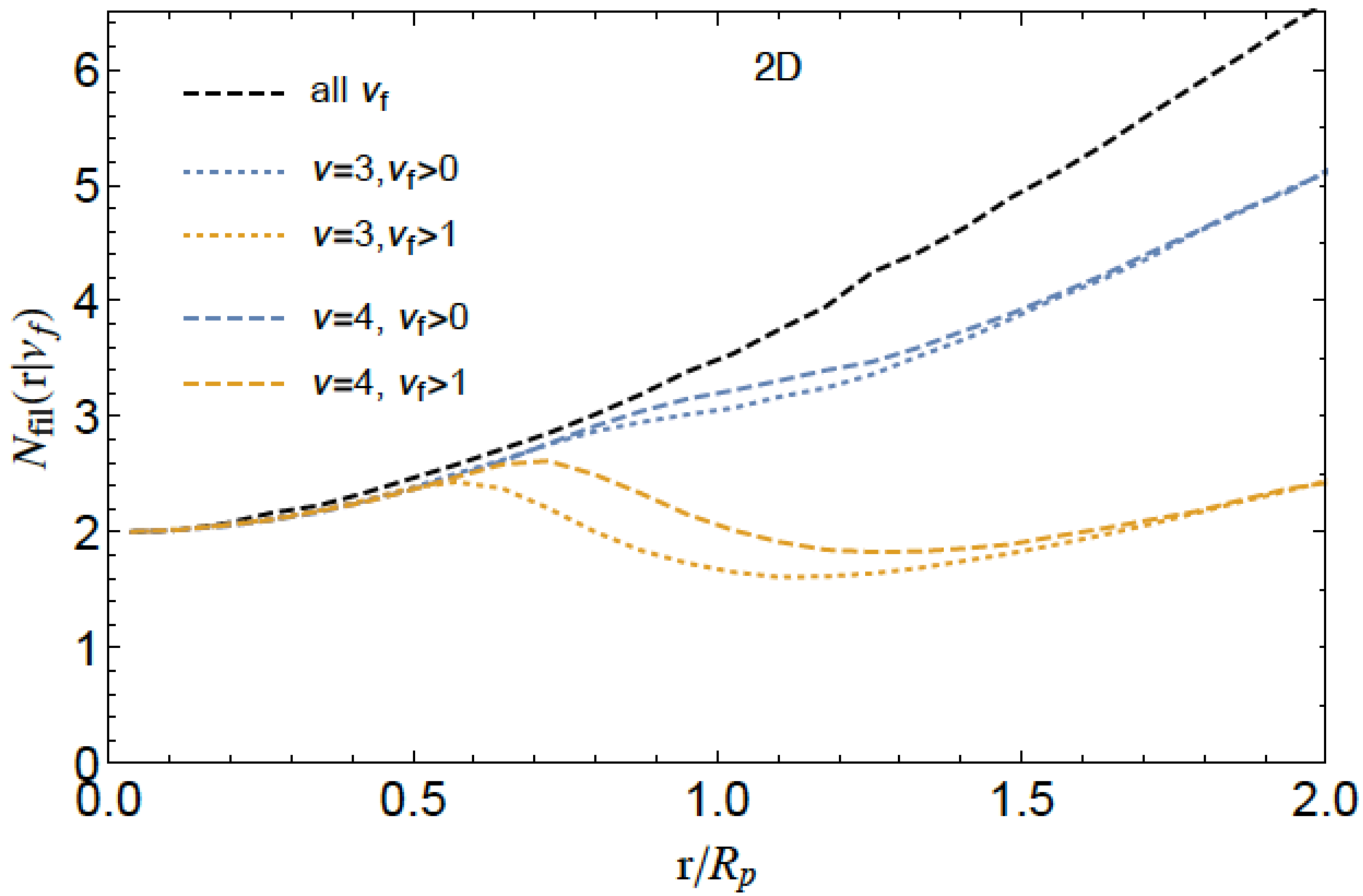

Typically, two to three dense filaments dominate and therefore define a **plane of accretion**… in agreement with numerical simulation (Danovich+12) and observations of plane of satellites around galaxies.

Conclusion

- Peak and constrained random field theories are paramount to understand the birth and growth of the cosmic web

- Many analytical results can be obtained in the weakly non-linear regime

- The topology and geometry of the cosmic web carries important cosmological information and is key for galaxy evolution.

- In particular, we now have a precise understanding of the connectivity of the cosmic web (the cosmic crystal)

horizon-AGN

Local multiplicity: towards a theoretical prediction